ORNL/TM-10985

ornl

OAK RIDGE
NATIONAL
LABORATORY

MARTIN MARIETTA

Shield Optimization Program, Part III: Effects of X-Ray Radiation From Nuclear Weapons on SDI Weapon Platforms

J. O. Johnson
T. A. Gabriel
J. M. Barnes
J. D. Drischler
M. S. Smith
R. T. Santoro

OPERATED BY
MARTIN MARIETTA ENERGY SYSTEMS, INC.
FOR THE UNITED STATES
DEPARTMENT OF ENERGY

Printed in the United States of America. Available from
National Technical Information Service
U.S. Department of Commerce
5285 Port Royal Road, Springfield, Virginia 22161
NTIS price codes—Printed Copy: A05 Microfiche A01

ORNL/TM-10985

Engineering Physics and Mathematics Division

Shield Optimization Program, Part III: Effects of X-Ray Radiation From Nuclear Weapons on SDI Weapon Platforms

J. O. Johnson, T. A. Gabriel, J. M. Barnes,*
J. D. Drischler, M. S. Smith, and R. T. Santoro

Date Published - March 1989

*Computing and Telecommunications Division

Prepared by the
OAK RIDGE NATIONAL LABORATORY
Oak Ridge, Tennessee 37831
operated by
MARTIN MARIETTA ENERGY SYSTEMS, INC.
for the
U.S. DEPARTMENT OF ENERGY
under contract DE-AC05-84OR21400

PREFACE

The research reported here was performed for the Air Force Weapons Laboratory (AFWL) in support of the Strategic Defense Initiative (SDI) Passive Survivability Technology Program.

The natural and man-made radiation environments of space pose significant potential threats to space deployed SDI systems. The data reported here are the results of an initial study to parameterize the radiation induced damage to silicon based electronic components carried on a Space Based Interceptor (SBI) weapon platform due to blackbody X-ray radiation emanating from a nuclear weapon detonation in space. The calculations performed in this study were carried out using three-dimensional radiation transport methods and an Oak Ridge National Laboratory (ORNL) conceptual model of a representative SBI weapon platform architecture.

Subsequent studies will be made to parameterize the effects of the various shielding and hardening techniques currently being considered in the SDI Survivability Program and more rationally isolate the significant radiation induced damage thresholds due to nuclear weapon X-rays. Furthermore, the study presented here and the subsequent studies will be extended to a representative Space Surveillance and Tracking System (SSTS) satellite architecture.

CONTENTS

LIST OF FIGURES

LIST OF TABLES

Table		Page

ABSTRACT

Initial studies have been completed to estimate the radiation induced damage to the silicon based electronic components and other sensitive areas (fuel tanks) carried on a representative Space Based Interceptor (SBI) weapon platform. The SBI weapon platform model used in the studies represents the author's concept of such a system. The analysis was completed for the blackbody X–ray radiation environment emanating from a nuclear weapon detonation in space and considered blackbody temperatures in the range of 1 to 25 keV and exterior wall loadings in the range of 1 to 10 cal/cm^2.

The results indicate the dose to the sensitive components within the exterior hull of the platform was insufficient to cause any damage at a 1 to 3 cal/cm^2 exterior wall loading. At higher (5 to 10 cal/cm^2) exterior wall loadings, some of the Kinetic Kill Vehicle (KKV) computers and sensors begin to receive doses sufficient enough to cause damage. The effects of shielding from within the platform architecture is seen by the different dose levels received in the KKVs and fuel tanks. Because of the low dose levels to the components within the exterior hull of the platform, no additional shielding is required for these components and for low exterior wall loadings. However, sensors and electronic components on the surface or outside of the exterior hull will require some form of X–ray shielding to survive the effects of a nuclear weapon detonation yielding a wall loading of 1 cal/cm^2 or greater. All of the calculations were carried out for an unshielded SBI weapon platform to determine the radiation levels for which shielding must be designed to insure survivability of the electronic systems.

1. INTRODUCTION

Electronic equipment, especially modern integrated circuits, when exposed to various radiation environments will undergo an alteration of the electrical properties of the active components. The various natural and man–made radiation environments include Van Allen belt protons and electrons; galactic and solar flare protons; neutrons, gamma rays, and X–rays from fission and fusion weapons; and directed neutral particle beams and lasers. The changes in the electrical properties can result in degradation of circuit performance or temporary or permanent circuit failure. Furthermore, in a pulsed radiation environment, radiation induced photo currents can lead to transient circuit upsets.[1]

The Optimization Program was initiated to optimize nuclear performance of shields. Space-based interceptor (SBI) and Space Surveillance and Tracking Systems (SSTS) are studied since they have need for advanced kinetic energy weapon (KEW) and laser shielding. Studies of the nuclear environment and its effects on the Strategic Defense Initiative (SDI) platforms and shielding are required so that the benefits of added shielding can be determined and application methods, materials, and shield designs can be identified which optimize the shields survivability and the shields nuclear mitigation capability. In the future, the SSTS platform and more realistic SBI orbital inclinations will be studied with various levels of added KEW shielding and applied optimization techniques.

The purpose of this work was to determine the dose to the various electronic components and sensitive areas (fuel tanks) of a representative Space Based Interceptor (SBI) weapon platform due to a nuclear weapon X–ray radiation environment. A nuclear detonation will heat the device and surrounding materials to tens of millions of degrees Kelvin. Due to this high temperature, blackbody radiation will occur in the form of X–ray radiation. Approximately 75% of the total energy emitted during a detonation will appear in the form of X–rays.[2] If the detonation occurs in the atmosphere, the X–ray radiation will be reduced rapidly due to absorption in the air and the geometric ($1/R^2$) divergence. In space, however, only geometric divergence is initially available and consequently a weapon platform could receive X–ray fluences sufficient enough to cause damage to the electronics and sensitive areas on the platform.

A second purpose was to determine if there is a requirement for shielding around the sensitive electronic components to reduce the dose to electronics systems. Shielding of the electronic equipment can minimize damage received and will allow for extended lifetimes of the equipment and allow the platform to complete its mission requirements.

Damage levels are characterized by several parameters depending on the radiation considered. The parameter utilized in this work is the total energy deposition – rads(Si).

Presented in Section 2 of this report are the SBI weapon platform geometry model, the blackbody X–ray source spectra, and the codes, analysis routines, and weapon detonation scenarios used in these calculations; in Section 3, the discussion of the calculated results; and in Section 4, a summary.

2. METHOD OF CALCULATION

2.1 SPACE BASED INTERCEPTOR PLATFORM MODEL

A computer model of a typical Space Based Interceptor (SBI) weapon platform has been devised to estimate the effects of natural and nuclear weapon radiation on the external surfaces and materials and on the internal components. The external surfaces include the platform structure, kinetic energy and laser weapon shields, solar panels, antenna, etc. The internal components include electronic modules and circuits, sensors, interceptors, fuel, etc. Design details not relevant to the dose calculations have been omitted or purposely neglected in order to optimize the computational effort. The platform configuration adopted for this analysis is shown in Fig. 1. A brief description of the ORNL SBI weapon platform is given below. A more detailed description is given in Reference 3.

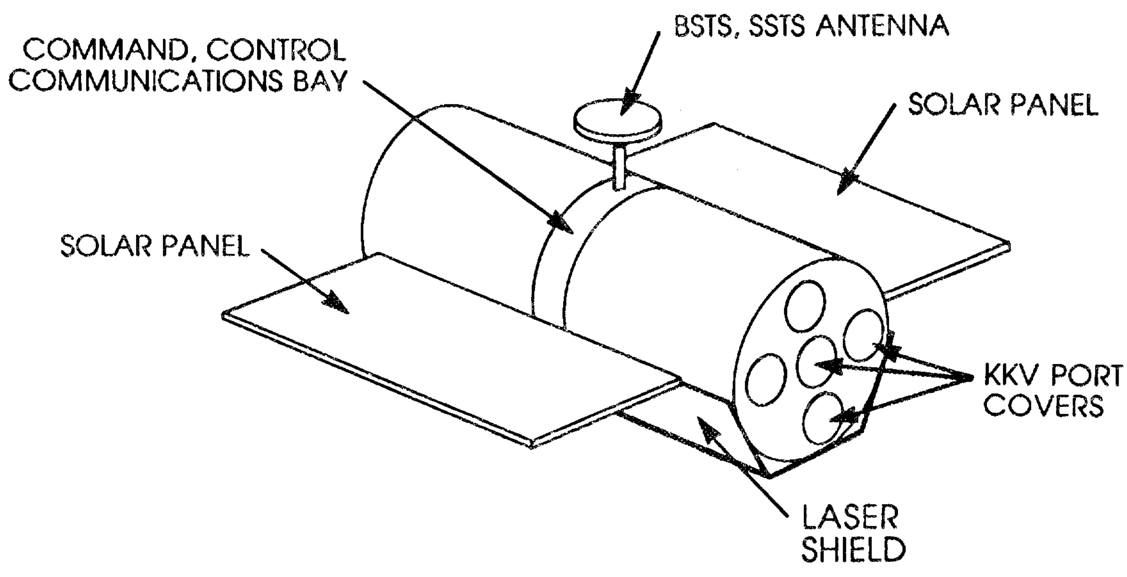

Figure 1. Space Based Interceptor Weapon Platform.

It should be noted that the SBI weapon platform used in this study represents the author's concept of such a system and is not that proposed for deployment by the Strategic Defense Initiative Organization (SDIO). The platform was "designed" on the basis of space weapon system requirements eluded to in the Defense Acquisition Board documentation on SDI space weapon–sensor architecture requirements. Design guidance was also taken from briefings by other institutions also involved in weapon platform studies. In developing the platform representation shown in Fig. 1, every effort has been made to protect proprietary information and configurations.

2.2 THE SBI PLATFORM GEOMETRY

The ORNL weapon platform is a cylindrical shell comprised of two modules containing the platform fuel tanks and the Kinetic Kill Vehicle (KKV) launch tube assemblies connected by a command, control, and communications (C^3) bay. Each module contains five KKV launch tube assemblies and four fuel tanks. A cut–away view of the interior of the platform is provided in Figs. 2 and 3. Shown in these figures are the fuel tanks located between the KKV launch tube assemblies and on the same radius as the launch tubes (Fig. 2), and the details of two KKV launch tube assemblies with the KKVs shown in place(Fig. 3). The fuel is intended for maneuvering the platform to avoid collisions with space debris, evade enemy kill vehicles, and position the platform during an engagement.

Power is supplied to the platform by solar panels shown in the deployed position in Fig. 1. A single antennae is shown, but it is recognized that other antenna and sensors may also exist on an actual platform design. A laser weapon shield covers the earth exposed surfaces for protection against illumination by ground based laser weapons. As presently configured, the overall dimension of the laser weapon shield may not assure sufficient attenuation of laser radiation thermal loading on the outer surface of the SBI vessel. Initially, kinetic energy weapon shielding will not be included as part of the platform. Omission is for two reasons: (1) uncertainty in the positioning of these shields, i.e., directional or full coverage and (2) to obtain data on the radiation response of components and surface materials and hardening requirements for the platform itself.

Figure 4 shows the command, control, and communications bay. The electronic circuits are housed in two concentric ring assemblies. At the center of the module is a "critical components" box. The cylindrical ring assemblies and the box are thin walled hollow assemblies that can be filled with detailed models of electronic circuitry or homogenized materials representative of those comprising the electronic packages. The electronics bay is also designed for incorporating additional shielding should it be necessary to further minimize the effects of radiation.

Figure 5 shows the details of a Kinetic Kill Vehicle (KKV). Ten identical KKVs are modeled in their appropriate locations inside the platform. The principal components of each kill vehicle include the warhead, sensors, computers, fuel tank, and rocket motor. The body of the interceptor will contain appropriate shielding (hardening) to protect the interceptor guidance system and other critical electronic components necessary for mission success from exposure to weapon radiation outside of the platform during engagement.

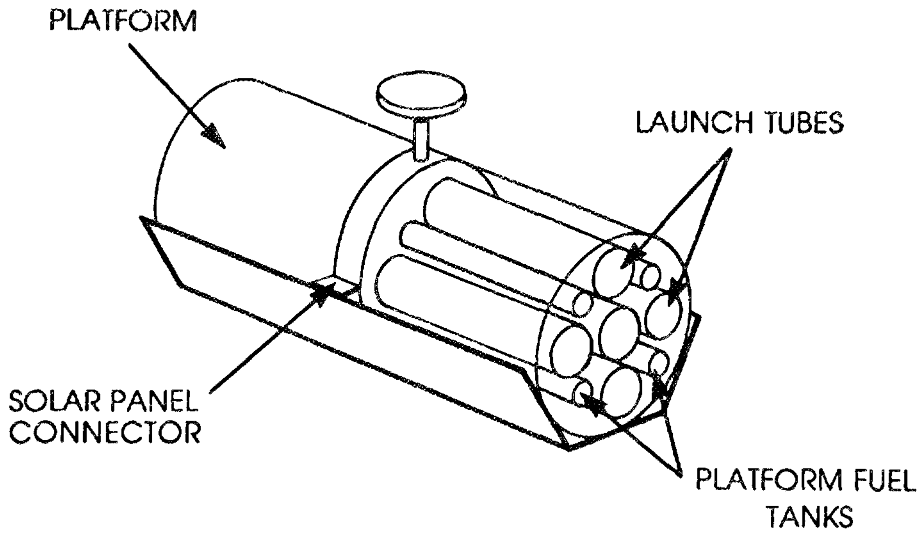

Figure 2. Cut-away view of SBI Weapon Platform showing relative positions of KKV launch tubes and platform fuel tanks.

2.3 THE SBI PLATFORM MATERIALS

The SBI Platform is currently configured to have a weight of $\approx$ 2030 kg, not including the ten KKVs that it will carry. A description of the material composition is given in Table 1. The laser shield material has been taken to be carbon of theoretical density and is probably too thin to be effective in reducing the laser weapon thermal loads to the skin of the SBI platform. However, for the purpose of initial calculations, this is sufficient.

Currently, there is no additional internal shielding in place to reduce the effects of natural and nuclear weapon radiation environments to the electronic components. The electronics are represented as homogeneous silicon distributed throughout the instrument bay at theoretical or reduced density depending on the location in the platform.

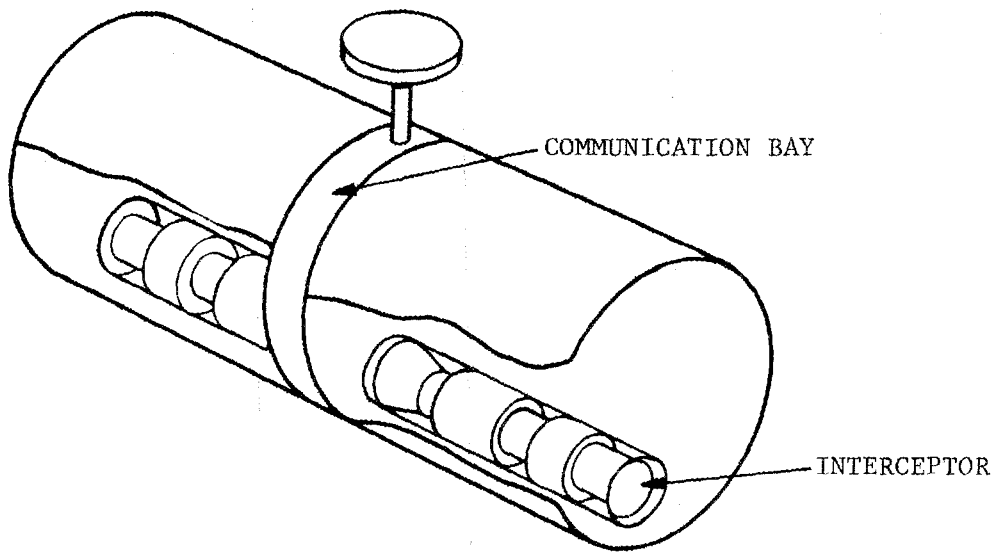

Figure 3. Cut-away view of SBI Weapon Platform showing two KKV launch tubes and platform instrument bay.

The fuel carried in the platform for evasive maneuvers is presently taken to be hydrazine having a density of 1.0 g/cm^3. The quantity of fuel was arbitrarily chosen to maintain the overall weight of the SBI weapon platform.

2.4 THE KKV MATERIALS

Table 2 lists the materials and weights of the KKV components depicted in Fig. 5. These were selected to obtain a vehicle weight of $\approx$ 69 kg (152 lbs). The KKV sensors and computers are initially unshielded in order to assess their vulnerability to the incident radiation. These components will be hardened using reentry vehicle hardening technology to assure survivability in severe nuclear radiation environments.

2.5 BLACKBODY X–RAY SPECTRA

To examine the effects of a blackbody X–ray radiation environment, calculations at a variety of temperatures (cold $\lesssim$2 keV, hot $\gtrsim$2 keV) were considered. The

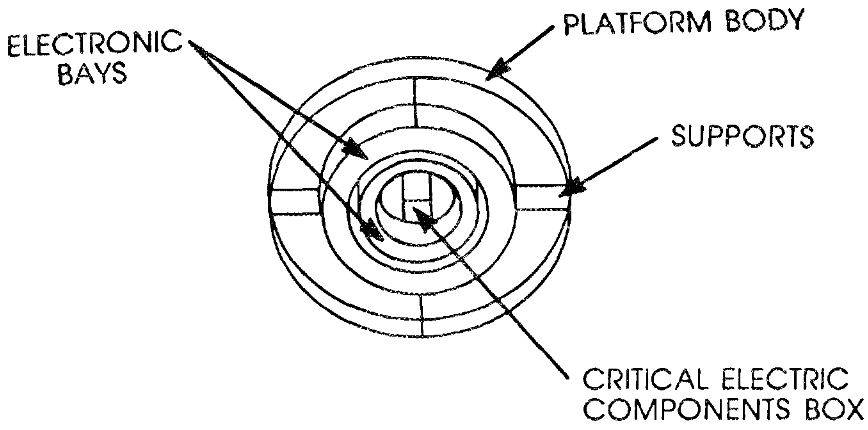

Figure 4. Instrument bay.

differential energy distribution (X–rays/unit energy) associated with blackbody X–rays can be written

$$\frac{dN(E,kt)}{dE} = \frac{CE^2}{e^{E/kT} - 1}$$

where N is the number of X–rays with energy E about dE, kT is the temperature of the emitting object, and C is a normalization factor.[4] A plot of this distribution is given in Fig. 6 for various kT values: 1, 2, 5, 10, 15, 20, and 25 keV. As the temperature of the blackbody radiator increases, the emission spectrum hardens. For the temperatures shown, the average energy of an emitted X–ray is 2.66, 5.38, 13.5, 27.0, 40.4, 53.9, and 67.4 keV. The blackbody X–ray calculations were performed so that the effects of an arbitrary X–ray spectrum can be created. To allow construction of a blackbody radiation spectrum representative of a nuclear weapon detonation, temperatures (kT) of 2, 5, 10, and 20 keV were used. Surface loadings in the range of 1–10 cal/cm^2 were considered.

2.6 NUCLEAR WEAPON DETONATION SCENARIOS

To accommodate the directional source spectra incident on the SBI platform from a nuclear detonation, three scenarios were considered in the analysis. The first scenario modeled the nuclear detonation directly above the SBI platform, the second scenario modeled the nuclear detonation directly in front of the SBI platform, and the third scenario modeled the nuclear detonation incident on the top and front face of the platform at a 45 degree angle. The nuclear weapon detonation was modeled

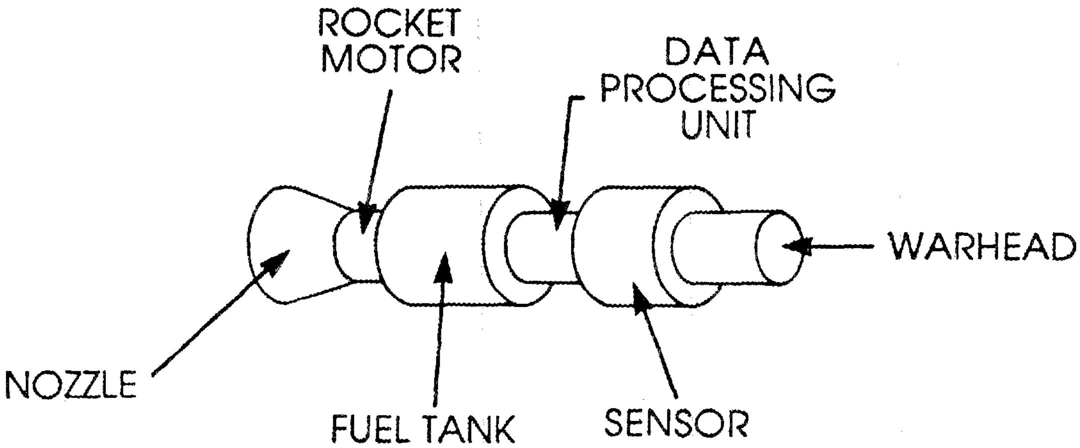

Figure 5. Kinetic kill vehicle.

such that the incident radiation spectra could be assumed monodirectional. Fig. 7 illustrates the positions of the three nuclear weapon detonations relative to the SBI platform.

2.7 RADIATION TRANSPORT ANALYSIS DETECTOR REGIONS

The current analysis routines calculate the dose to those areas of the platform which contain electronic components or materials which may be sensitive to radiation damage. To accommodate directional source spectra, such as that from a nuclear detonation, 68 different detector regions have been identified. The term detector in this context is used to identify a region in the radiation transport geometry model for which a response is desired. In particular, the Command, Control, Communications (C^3) Bay contains 15 detector regions. These include the critical electronic component box in the center of the C^3 Bay, six angular segments for the inner electronic bay ring, and eight angular segments for the outer electronic bay ring. A schematic diagram detailing the C^3 Bay detector region

Table 1

Material Compositions for the SBI Weapon Platform

Component	Vol. (cm^3)	Material	Wt. (kg)
Solar Panel	291,350.76	Be-Si	552.11[a]
Solar Panel Connector	1,524.00	Al	4.11
Antenna Support	3,926.99	Al	10.60
Antenna	38,484.51	Si	17.70[b]
Laser Shield	111,929.95	C	223.86
Platform (2 parts)	39,484.51	Al	106.61
	39,484.51	Al	106.61
Instrument Bay Housing	18,273.98	Al	49.34
Instrument Bay Box	6,021.32	Si	2.77[b]
Instrument Bay Walls	692.68	Al	1.87
Most Inner Circle Instrument Bay Wall	1,509.52	Al	4.08
Circular Instrument Bay (Inner)	52,647.26	Si	24.22[b]
Circular Instrument Bay Wall (Inner)	2,090.30	Al	5.64
Circular Instrument Bay Wall (Outer)	2,409.47	Al	6.51
Circular Instrument Bay (Outer)	127,887.01	Si	58.83[b]
Circular Instrument Bay Wall (Outer)	3,290.23	Al	8.88
Circular Instrument Bay Support (4 Posts)	201.83	Al	2.18
KKV Tube (10)	8,158.08	Al	220.27
Fuel Tank (8)	2,143.30	Al	46.30
Fuel	64,145.11	N_2H_4	513.16
Platform Support Beams (16)	1,225.41	Al	52.94
KKV Tube Caps (10)	428.27	Al	11.56
		Total Weight	2030.15

[a]90% Beryllium – 10% Silicon (at 50% Density)
[b]Silicon at 20% Density.

Table 2

Material Compositions for the Kinetic Kill Vehicles (Per KKV)

Component	Vol. (cm^3)	Material	Wt. (kg)	
Nozzle	2,148.04	CC	4.30	
Motor Housing	635.73	Al	1.72	
KKV Motor	8,748.33	SS	10.24	(15%)
Fuel Tank	2,602.52	Al	7.03	
Fuel	54,850.93	N_2H_4	13.71	(25%)
Computer Housing	1,224.44	Al	3.31	
Computer	9,423.26	Si	4.33	(20%) See Note A
Sensor Housing	1,994.59	Al	5.39	
Sensor	20,023.96	Si	9.21	(20%)
KKV Warhead	1,271.65	SS	9.92	
Total Weight			69.16	

KKV Warhead L/D = 2.0 = (18.64/9.32).
KKV Motor at 15% Density to Account for Structure.

Note A: Must ultimately insert a box inside this volume for housing a "computer."

numbering system used in the analysis routines is shown in Fig. 8. The angular segmenting of the electronic bay rings will identify variations in the dose due to any inherent shielding designed into the platform. This will be important when considering directional source spectra. There are ten kinetic kill vehicles (KKVs) onboard the platform, each with a computer and sensor region and a fuel tank. The Hydrazine fuel was considered because of possible radiation damage causing material breakdown of the fuel components. For the same reasons stated above, each computer, sensor, and fuel tank has been identified as a separate detector region. The solar panels have been modeled as two separate detector regions. Furthermore, since the solar panels are on the exterior of the platform and directly exposed to the incident radiation, each panel has been subdivided into five additional detector regions to calculate dose profiles in the solar panels and identify potential surface phenomenology, i.e. blow off, melting, etc. A schematic diagram detailing the solar panel region numbering system used in the analysis routines is shown in Fig. 9. Similar to the solar panels, the Boost Surveillance and Tracking System (BSTS), Space Surveillance and Tracking System (SSTS) antenna has been modeled as a separate detector region and it also has been subdivided into five additional detector regions to calculate dose profiles in the antenna and identify potential surface phenomenology. Finally, the eight SBI platform fuel tanks have been modeled as

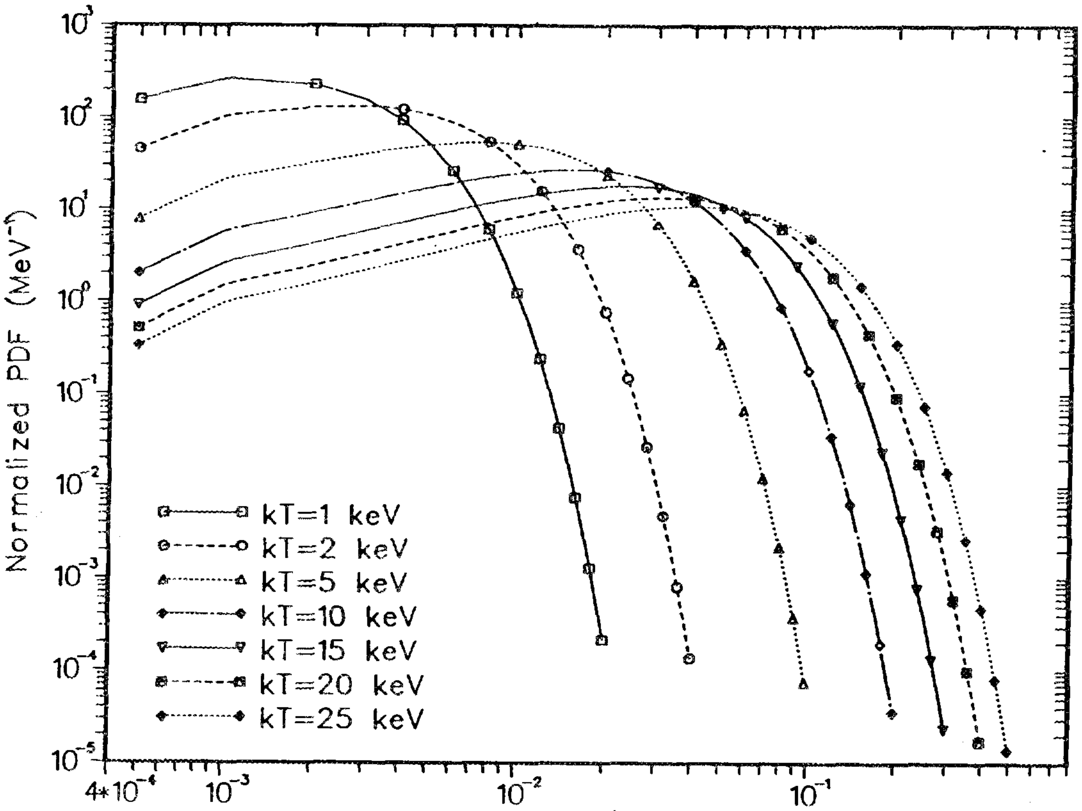

Figure 6. Blackbody X-ray spectra for various *kT* values.

separate detector regions. A schematic diagram detailing the Kinetic Kill Vehicle and SBI fuel tank numbering system used in the analysis routines and identifying the other detector regions is shown in Fig. 10. Furthermore, Table 3 equates the SBI weapon platform component with the detector region number in the radiation transport analysis.

2.8 RADIATION TRANSPORT CODES AND PROCEDURE

To accomplish the objectives mentioned earlier, the SBI platform geometry (Figs. 1–5), material compositions (Table 4), and analysis routines have been incorporated into the Electron Gamma-Ray Shower Code EGS4.[5] EGS4 is a three-dimensional multimedia transport code that can operate with the combinatorial geometry package. EGS4 takes into account all important physical processes including the photoelectric effect, positron annihilation, bremsstrahlung, pair production, compton scattering, and energy loss and directional changes associated

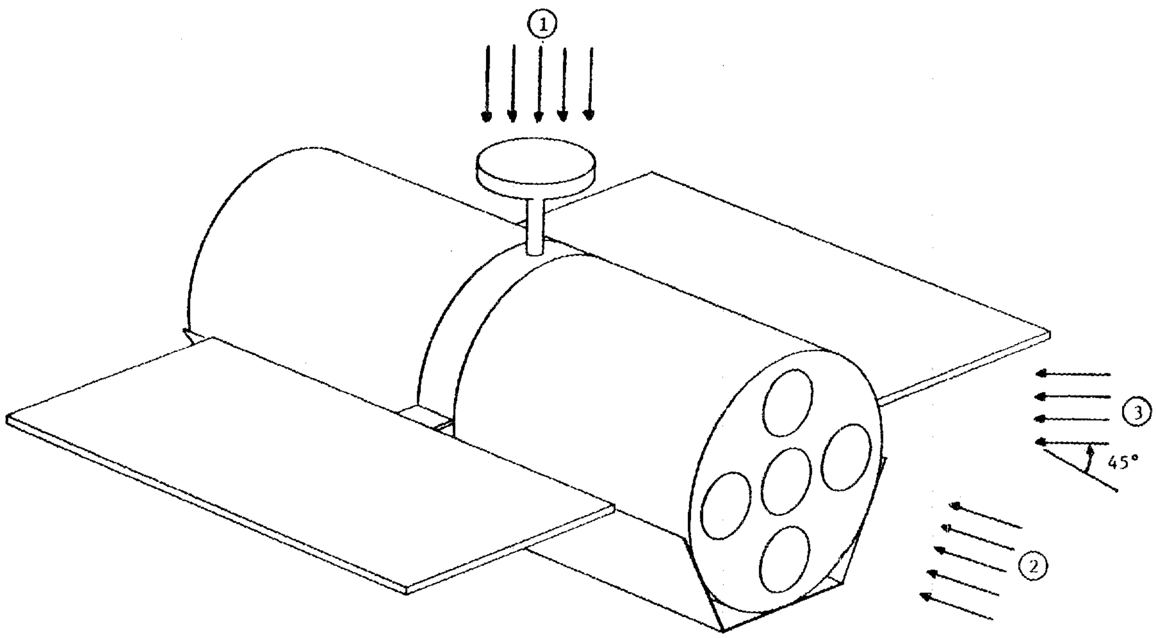

1. Incident on Top of SBI Platform
2. Incident on Front of SBI Platform
3. Incident on Front and Top at 45° Angle

Figure 7. Schematic diagram of the Spaced Based Interceptor Weapon Platform depicting directions of incident nuclear weapon source spectra.

Table 3

The Detector Regions Implemented in the Radiation Transport Analysis Routines

SBI Platform Component	Detector Region
C^3 Bay Critical Components Central Instrument Box	1
C^3 Bay Inner Instrument Ring	
0 to 60 Degree Segment	2
60 to 120 Degree Segment	3
120 to 180 Degree Segment	4
180 to 240 Degree Segment	5
240 to 300 Degree Segment	6
300 to 360 Degree Segment	7
C^3 Bay Outer Instrument Ring	
0 to 45 Degree Segment	8
45 to 90 Degree Segment	9
90 to 135 Degree Segment	10
135 to 180 Degree Segment	11
180 to 225 Degree Segment	12
225 to 270 Degree Segment	13
270 to 315 Degree Segment	14
315 to 360 Degree Segment	15
Kinetic Kill Vehicle Computers	
KKV Number 1	16
KKV Number 2	17
KKV Number 3	18
KKV Number 4	19
KKV Number 5	20
KKV Number 6	21
KKV Number 7	22
KKV Number 8	23
KKV Number 9	24
KKV Number 10	25
Kinetic Kill Vehicle Sensors	
KKV Number 1	26
KKV Number 2	27
KKV Number 3	28
KKV Number 4	29
KKV Number 5	30
KKV Number 6	31
KKV Number 7	32
KKV Number 8	33
KKV Number 9	34
KKV Number 10	35

Table 3 – Continued

SBI Platform Component	Detector Region
Right Solar Panel	
Inner 0.5 cm Thick Shell	36
Next 0.5 cm Thick Shell	37
Next 0.5 cm Thick Shell	38
Next 0.5 cm Thick Shell	39
Outer 0.5 cm Thick Shell	40
Left Solar Panel	
Inner 0.5 cm Thick Shell	41
Next 0.5 cm Thick Shell	42
Next 0.5 cm Thick Shell	43
Next 0.5 cm Thick Shell	44
Outer 0.5 cm Thick Shell	45
BSTS, SSTS Antenna	
Inner 1.0 cm Thick Shell	46
Next 1.0 cm Thick Shell	47
Next 1.0 cm Thick Shell	48
Next 1.0 cm Thick Shell	49
Outer 1.0 cm Thick Shell	50
Kinetic Kill Vehicle Rocket Fuel Tanks	
KKV Number 1	51
KKV Number 2	52
KKV Number 3	53
KKV Number 4	54
KKV Number 5	55
KKV Number 6	56
KKV Number 7	57
KKV Number 8	58
KKV Number 9	59
KKV Number 10	60
SBI Weapon Platform Rocket Fuel Tanks	
SBI Tank Number 1	61
SBI Tank Number 2	62
SBI Tank Number 3	63
SBI Tank Number 4	64
SBI Tank Number 5	65
SBI Tank Number 6	66
SBI Tank Number 7	67
SBI Tank Number 8	68

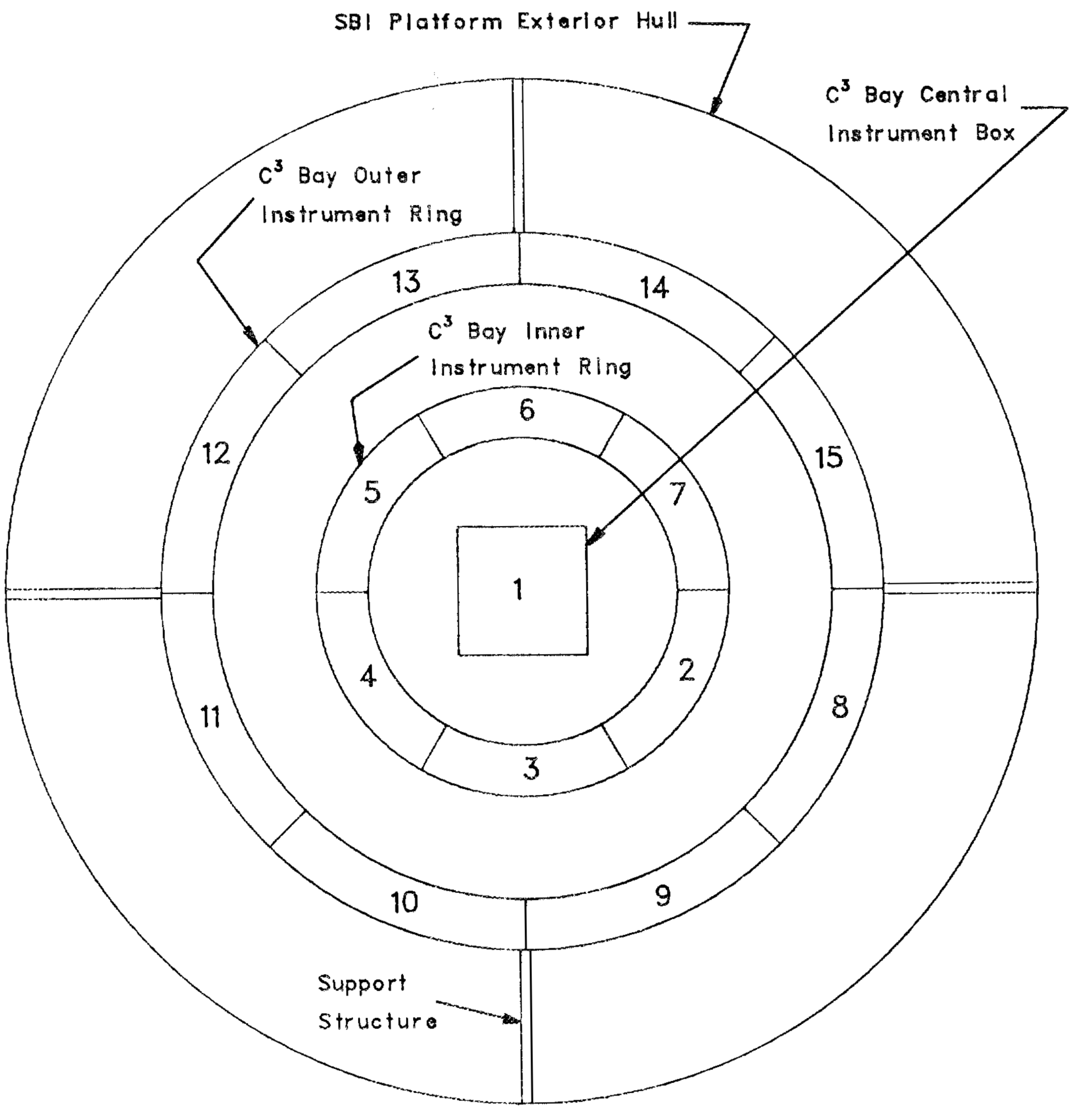

Figure 8. Schematic diagram of the Spaced Based Interceptor Weapon Platform Command, Control, Communications (C^3) Bay detailing the detector region numbering system used in the radiation transport analysis.

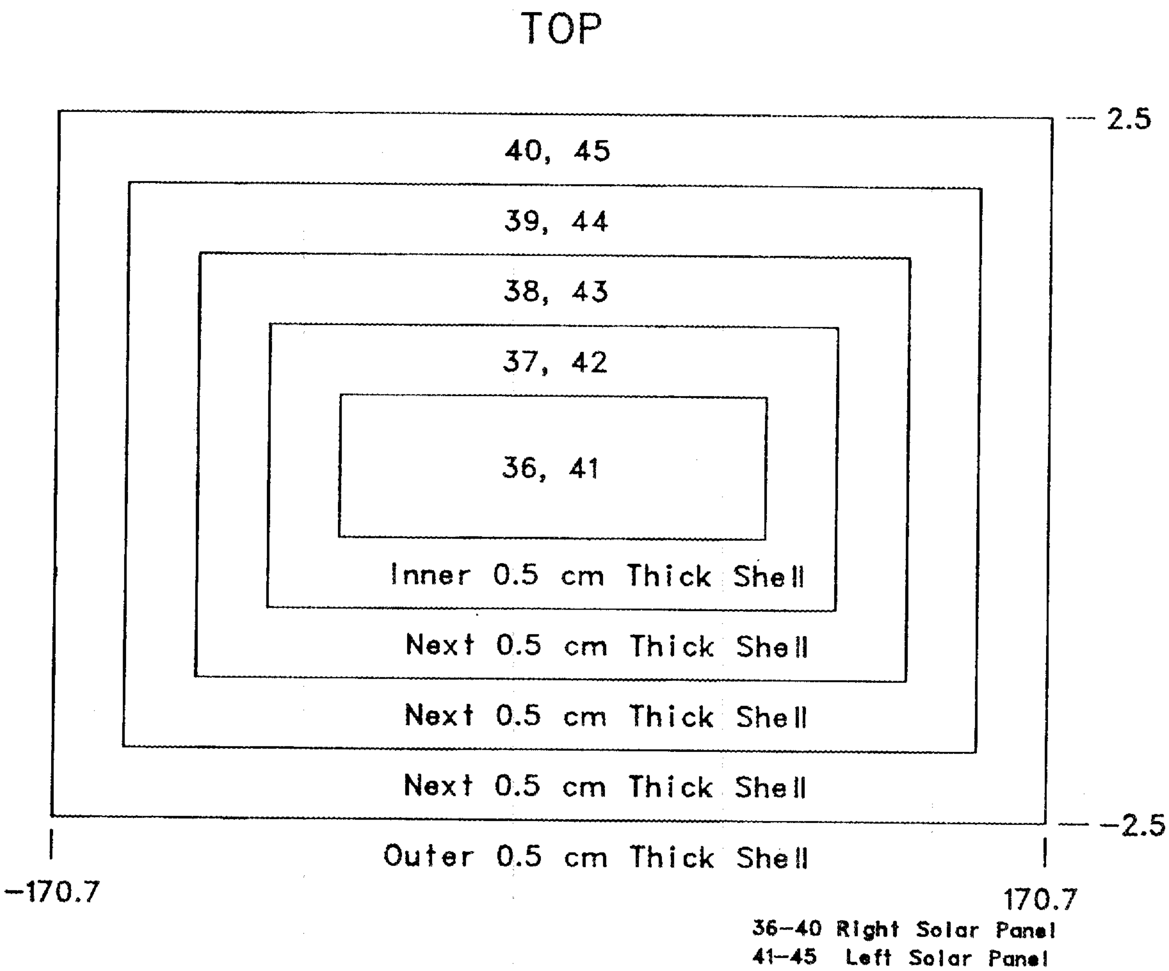

Figure 9. Schematic diagram of the Space Based Interceptor Weapon Platform solar panels detailing the detector region numbering system used in the radiation transport analysis.

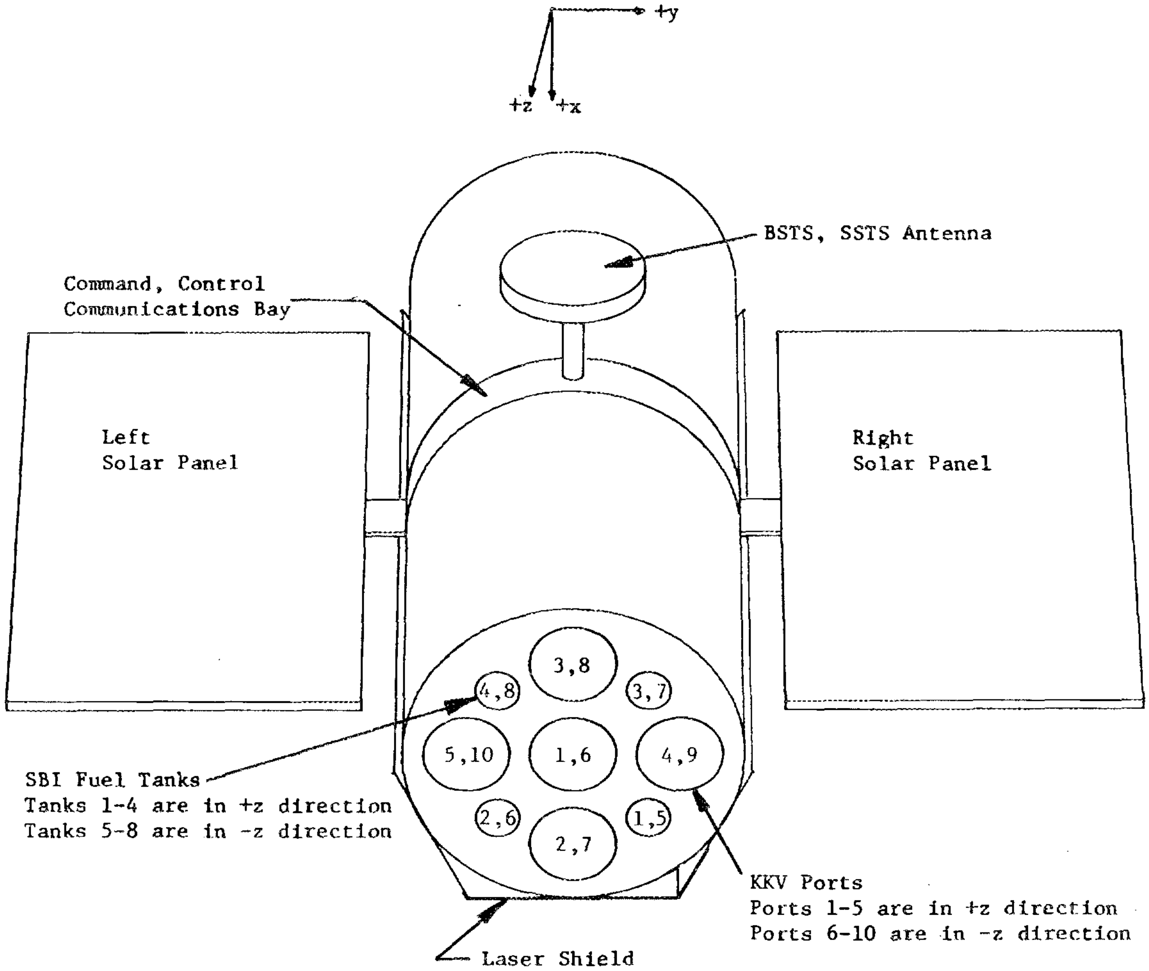

Figure 10. Schematic diagram of the Spaced Based Interceptor Weapon Platform detailing the kinetic kill vehicle and fuel tank numbering system used in the radiation transport analysis.

with electron and positron ionization excitation collisions with other electrons and nuclei. While primarily an analog Monte Carlo code, there are new features associated with this code which will be advantageous for future design calculations, including path length stretching and leading particle biasing. The EGS4 pre-processing program PEGS[5] is used to generate the necessary total and differential cross-section data. An added feature to the EGS4 code at ORNL is the coupling of the code to the other radiation transport codes used in the analysis of the SBI weapon platform.[6]

The blackbody X-ray source spectra at various temperatures were analyzed using EGS4 to calculate the energy deposition (dose) in the electronic components and sensitive areas due to the three nuclear weapon detonation scenarios mentioned above. To reduce computational effort and improve the accuracy of the results, the calculations were divided into source spectra incident on the platform body and source spectra incident on the solar panels. For the platform body, the EGS4 calculations analyzed 30 batches of 10,000 particles and for the solar panels, the calculations analyzed 10 or 20 batches of 2,000 particles depending on the temperature of the incident X-ray spectrum. Also, for the solar panels, only the weapon detonation directly above the platform was analyzed. The principal reason for this was because the surface area irradiated by the detonation at a 45 degree angle was similar to that for the detonation directly above the platform, and the surface area irradiated by the detonation directly in front of the platform was insignificant.

Table 4

SBI Platform and KKV Material Parameters

Component	Density (g/cm^3)	Weight Fraction	Atomic Weight	Atom Density $(barn \cdot cm)^{-1}$
Aluminum	2.70	1.00 Al	26.98	6.027–02[a]
Silicon @ 20%	0.46	1.00 Si	28.09	9.865–03
Hydrazine @ 25%	0.25	0.874 N	14.01	9.411–03
		0.126 H	1.01	1.882–02
Hydrazine	1.00	0.874 N	14.01	3.764–02
		0.126 H	1.01	7.529–02
Beryllium/Silicon @ 50%	0.95		9.01	5.564–02
			28.09	2.466–03
Graphite	2.00	1.00 C	12.01	1.003–01
Stainless Steel @ 15%	1.17	0.170 Cr	52.00	2.304–03
		0.017 Mn	54.94	2.181–04
		0.025 Mo	95.94	1.836–04
		0.120 Ni	58.70	1.441–03
		0.010 Si	28.09	2.510–04
		0.658 Fe	55.85	8.302–03
Stainless Steel	7.80	0.170 Cr	52.00	1.536–02
		0.017 Mn	54.94	1.454–03
		0.025 Mo	95.94	1.224–03
		0.120 Ni	58.70	9.604–03
		0.010 Si	28.09	1.673–03
		0.658 Fe	55.85	5.535–02
Air @ 10^{-10}%	1.22–03	0.756 N	14.01	3.965–17
		0.232 O	16.00	1.065–17
		0.012 Ar	39.95	2.355–19

[a]Read as 6.027×10^{-2}.

3. NUCLEAR WEAPON X-RAY RADIATION RESULTS

3.1 THE SOLAR PANEL RESULTS

The EGS4 results for the blackbody X–ray radiation environment incident on the solar panels are presented in Tables 5–7. Table 5 presents the total X–ray flux at 1 cal/cm^2 exterior wall loading for the various temperature blackbody sources analyzed. The solar panel results are presented in rads per unit flux (Table 6) and total rads (Table 7) at a 1 cal/cm^2 exterior wall loading for the various temperature blackbody spectra and for the weapon detonation directly above the platform. The weapon detonation directly in front of the platform was not analyzed for the solar panels because of the small cross sectional area presented to the incident source. Also, the weapon detonation at a 45 degree angle to the front and top faces of the platform was not analyzed for the solar panels because preliminary results indicated the weapon detonation directly above the platform sufficiently represented this scenario. The dose profile results in Tables 6 and 7 show several trends with respect to the temperature of the blackbody spectrum. The first obvious trend is the sharp decline in the dose profile for the lower temperature spectra (four orders of magnitude at 1 keV) and relatively flat dose profile for the higher temperature spectra (less than 20% at 20 keV). This is due to the shorter ranges of the X–rays for the lower temperature devices. The dose profiles in Table 7 are illustrated graphically in Fig. 11. Above 5 keV the dose profiles in Table 6 are relatively flat and of the same order of magnitude. However, in Table 7 the results show a decrease in the total dose because of the drop in the total X–ray flux incident on the solar panels (see Table 5). Because the detector regions were modeled as 0.5 cm thick concentric zones and treated as volume detectors in the radiation transport analysis (Fig. 9), the low temperature device results could underestimate the dose in the outer layer by a factor of two. This is due to the fact that the low energy X–rays will not penetrate the solar panel and deposit energy in the side away from the source. In Table 6, the peak dose is found in the outer shell of the solar panels (detectors 40,45) for the 5 keV blackbody spectrum. In Table 7, the peak dose is shown in the outer shell of the solar panels for the 1 keV blackbody spectrum. This again is due to the higher incident X–ray flux for lower temperature devices. The dose (Table 7) to the outer shell of the solar panels for the 1, 2, and 5 keV devices is sufficiently large enough to cause permanent damage to the solar panels. Further analysis with smaller thicknesses needs to be performed to determine the surface effects (blow–off, melting, etc.) present for the 1, 2, and 5 keV source spectra.

Table 5

The Average Energy and Total X-Ray Flux (at a 1 cal/cm^2 Exterior Wall Loading) for Various Temperature Blackbody X-Ray Sources

Temperature (keV)	Average Energy (MeV)	X-Ray Flux (X-Rays/cm^2)
1	2.657–03[a]	9.8329+15
2	5.379–03	4.8570+15
5	1.350–02	1.9353+15
10	2.701–02	9.6727+14
15	4.051–02	6.4493+14
20	5.402–02	4.8203+14
25	6.753–02	3.8688+14

[a]Read as 2.657×10^{-3}.

Table 6

Dose (in rads-cm^2/X-Ray) to the Solar Panels for Various Temperature Blackbody X-Ray Sources Located Directly Above the Solar Panels

Detector Region	Temperature of Blackbody Source						
	1 keV	2 keV	5 keV	10 keV	15 keV	20 keV	25 keV
36,41	4.634−17[a] ± 7.7[b]	8.301−15 ± 5.9	1.747−13 ± 2.2	3.413−13 ± 5.1	4.289−13 ± 4.1	4.036−13 ± 4.6	4.380−13 ± 3.
37,42	9.018−17 ± 7.5	1.285−14 ± 5.2	1.882−13 ± 2.4	3.651−13 ± 3.2	3.843−13 ± 4.4	4.432−13 ± 5.4	4.914−13 ± 3.
38,43	3.245−16 ± 5.2	2.188−14 ± 4.0	2.171−13 ± 2.3	3.850−13 ± 3.2	4.193−13 ± 3.8	4.538−13 ± 4.4	4.689−13 ± 4.
39,44	2.052−15 ± 3.6	6.090−14 ± 3.2	3.545−13 ± 1.9	4.388−13 ± 3.8	4.805−13 ± 3.5	4.805−13 ± 2.9	4.525−13 ± 3.
40,45	3.798−13 ± 0.6	7.426−13 ± 0.5	9.181−13 ± 1.0	5.873−13 ± 2.9	5.076−13 ± 3.6	5.024−13 ± 3.9	4.712−13 ± 3.

[a]Read as 4.634×10^{-17}.
[b]Percent Fractional Standard Deviation.

Table 7

Total Dose (in rads) to the Solar Panels for a 1 cal/cm^2 Wall Loading from Various Temperature Blackbody X-Ray Sources Located Directly Above the Solar Panels

Detector Region	Temperature of Blackbody Source						
	1 keV	2 keV	5 keV	10 keV	15 keV	20 keV	25 keV
36,41	4.556−01[a] ± 7.7[b]	4.032+01 ± 5.9	3.381+02 ± 2.2	3.301+02 ± 5.1	2.766+02 ± 4.1	1.952+02 ± 4.6	1.695+02 ± 3.
37,42	8.867−01 ± 7.5	6.243+01 ± 5.2	3.641+02 ± 2.4	3.531+02 ± 3.2	2.478+02 ± 4.4	2.143+02 ± 5.4	1.901+02 ± 3.
38,43	3.191+00 ± 5.2	1.063+02 ± 4.0	4.200+02 ± 2.3	3.724+02 ± 3.2	2.704+02 ± 3.8	2.195+02 ± 4.4	1.814+02 ± 4.
39,44	2.018+01 ± 3.6	2.958+02 ± 3.2	6.861+02 ± 1.9	4.244+02 ± 3.8	3.099+02 ± 3.5	2.324+02 ± 2.9	1.751+02 ± 3.
40,45	3.734+03 ± 0.6	3.607+03 ± 0.5	1.777+03 ± 1.0	5.681+02 ± 2.9	3.274+02 ± 3.6	2.430+02 ± 3.9	1.823+02 ± 3.

[a]Read as 4.556×10^{-1}.
[b]Percent Fractional Standard Deviation.

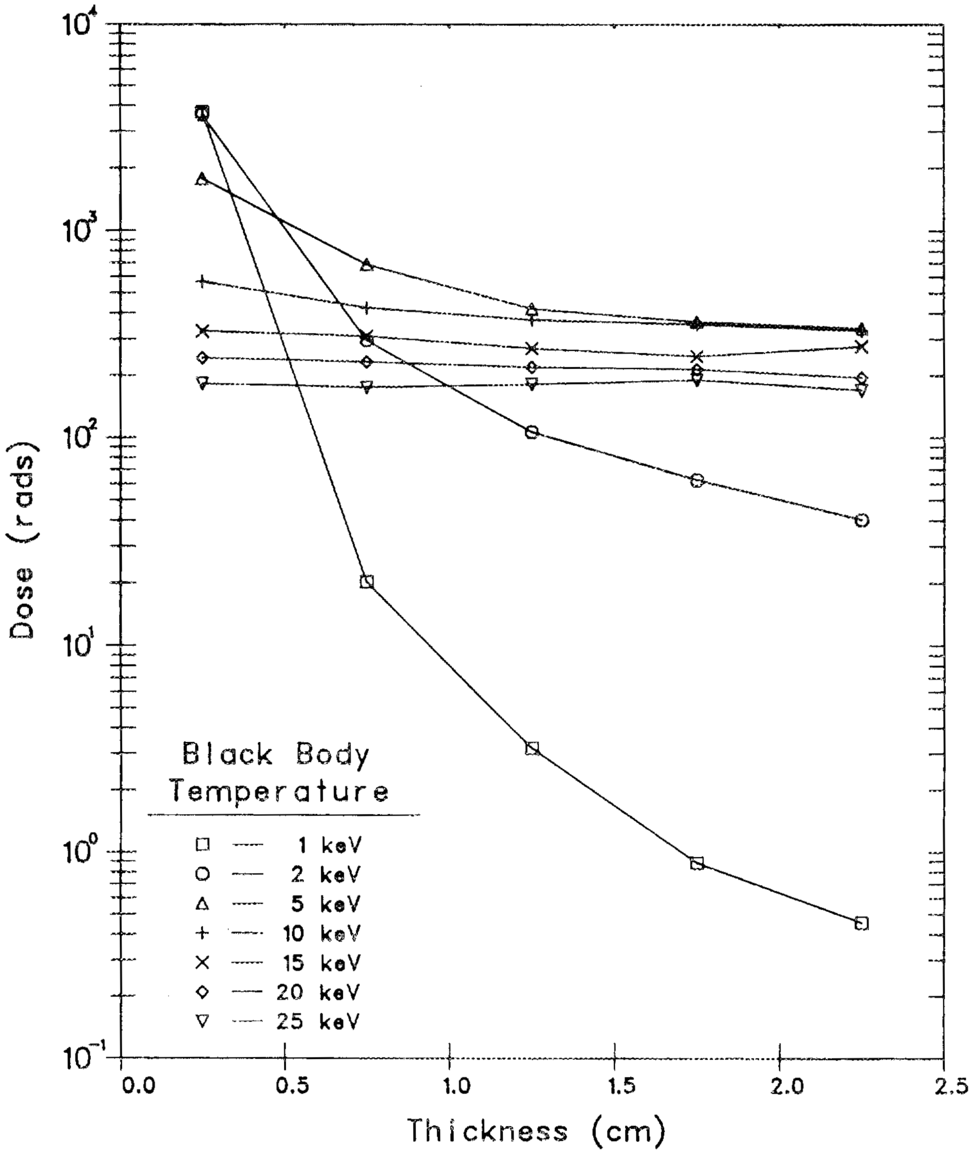

Figure 11. Dose versus depth into the solar panels as a function of blackbody temperature.

3.2 THE SBI PLATFORM BODY RESULTS

The results for the platform (including the solar panel results) are presented in Tables 8–22. Table 8 presents the dose results per unit flux for the 2, 5, 10, and 20 keV temperature blackbody spectra and for the weapon detonation directly above the platform. Tables 9–12 present the total dose results at 1, 2, 5, and 10 cal/cm^2 exterior wall loadings, for the 2, 5, 10, and 20 keV temperature blackbody spectra, and for the weapon detonation directly above the platform. Tables 13–17 and Tables 18–22 repeat the above sequence of results for the weapon detonation directly in front of the platform and for the weapon detonation at a 45 degree angle to the top and front faces of the platform respectively. *For the weapon detonation directly in front of the platform, the solar panel results (detectors 36–45) and the BSTS, SSTS antenna results (detectors 46–50) are from direct scattering of the incident radiation off of the platform, i.e., these regions were not modeled with the source incident upon them.* For the other two weapon detonation scenarios, the solar panel results for the platform have been summed with the results for the solar panels (Tables 6 and 7) to include the effects of secondary scattering. In the other detector regions, the secondary scattering contribution was insignificant and therefore was not included in the tables. Symmetry (with respect to the incident source) was utilized whenever possible to improve the statistics of the results. It should be noted that the fractional standard deviation (FSD) for some of the detector regions is large. In these cases, the results will indicate a relative magnitude of the dose and not an absolute quantity. To calculate these detector regions to within an acceptable FSD (±15%) would require considerable computational effort and would show that the doses to these detector regions are insignificant.

There is a considerable amount of data presented in Tables 8–22 and only a few general trends will be pointed out in this discussion. Also, unless otherwise stated, the results will be quoted for a 1 cal/cm^2 wall loading.

First, only the outer detector regions of the solar panels (detectors 40 and 45) and BSTS, SSTS antenna (detector 50) received sufficient dose to cause any temporary or permanent damage (dose greater than 10^3 rads) at a 1 cal/cm^2 wall loading. As stated earlier, these areas need to be analyzed using smaller thicknesses to determine how much of the total dose is a surface dose.

The Command, Control, Communications (C^3) Bay central instrument box received a maximum dose of 31 rads (Table 12, detector 1) for a 20 keV blackbody temperature weapon detonation directly above the platform and a 1 cal/cm^2 exterior wall loading. The angular segmenting of the C^3 Bay inner instrument ring (detectors 2–7) and outer instrument ring (detectors 8–15) shows the effects of shielding from within the platform architecture and also the importance of the location of a weapon detonation. The results for the weapon detonation directly above the platform (Tables 9–12) exhibits a factor of 2 difference in the doses received in the inner instrument ring angular segments (detectors 2–7) and a factor of 13 difference in the outer ring angular segments (detectors 8–15) for the 20 keV temperature device. The results for the detonation at a 45 degree angle to the top/front face of the platform (Tables 19–22) exhibit similar results with a factor of 5 difference in the doses received in the inner instrument ring angular segments (detectors 2–7) and a factor of 10 difference in the outer ring angular segments (detectors 8–15) for the 20 keV temperature device. The larger differences in the doses received in the inner ring angular segments can be attributed to the direct line of sight to the top portions of the C^3 Bay instrument inner ring for the detonation at the 45 degree angle to the top/front face of the platform. The results for the detonation directly in front of the platform (Tables 14–17) show a flat distribution of the dose in the angular segments of the instrument rings. The results also show a considerably higher dose in the inner instrument ring ($\approx$ 100 rads) than that received in the outer ring ($\approx$ 41 rads) or that received from either of the other two detonation scenarios for the 20 keV temperature device. The primary reason for both of the above trends is the direct line of sight of the X–rays from the detonation. The outer instrument ring is shielded by the KKVs and platform fuel tanks and therefore receives a lower dose for this scenario. In the other two scenarios, the outer instrument ring acts as a shield for the inner instrument ring and consequently receives the higher dose. None of the three weapon detonation scenarios analyzed in this work offered a direct line of sight to the (C^3) Bay central instrument box.

The results for the Kinetic Kill Vehicle computers (detectors 16–25), sensors (detectors 26–35), and fuel tanks (detectors 51–60), and the SBI platform fuel tanks (detectors 61–68) exhibit the same general trends mentioned above with respect to the different weapon detonation scenarios. The results for the weapon detonation directly above the platform (Tables 9–12) show differences of 10 to 15 in the dose for a particular component type, i.e., sensor, computer, etc., for the 20 keV temperature device. The shielding effects inherent in the platform design can be seen by comparing the dose received in the different KKV components and platform fuel tanks. For example, for the 20 keV temperature device (Table 12), the KKV computers (detectors 16–25) received a dose between 14 rads and 200 rads. The KKVs closest to the source (KKV 3 and KKV 8) received $\approx$ 200 rads. The KKVs in the center of the platform (KKV 1 and KKV 6) were shielded by the KKVs above them and received $\approx$ 46 rads. The KKVs on the bottom (relative to the source) of the platform (KKV 2 and KKV 7) were shielded by two sets of KKVs and received only $\approx$ 14 rads. The KKVs which were partially shielded by the platform fuel tanks (KKVs 4, 5, 9, and 10) received $\approx$ 105 rads. Similar results are seen in the other KKV components and the platform fuel tanks.

The results for the weapon detonation at a 45 degree angle to the top/front face of the platform (Tables 19–22) show similar results for a particular side of the platform (front or back) but also show a decrease in the dose between the front and back components in the same relative position in the platform architecture. The KKV computer (detectors 16–25) results for the 45 degree angle detonation scenario and 20 keV temperature device show differences on the order of a factor of 2 for KKV 1 and KKV 6 or KKV 2 and KKV 7, and very small differences for the other computers. The KKV sensor (detectors 26–35) results for the same detonation scenario show a factor of 5 difference between KKV 1 and KKV 6, a factor of 17 difference between KKV 2 and KKV 7, and only a 30% difference between the other sensors in the same relative position (front to back) in the platform architecture. The larger differences in the KKV sensor results are due to the direct line of sight the incident radiation has on the sensors in the front side of the platform. It should be noted that this effect is not seen in the sensor results for the two KKVs located in the top of the platform because there is no additional shielding offered by other platform components. In general, the doses received in the components from a

45 degree angle detonation are lower than the doses received in the components due to the detonation directly above the platform. Instances where this trend is not true are probably due to components directly illuminated by the incident radiation. The principal factor influencing the above results is the additional shielding offered by the KKVs and fuel tanks on the front side of the platform and by the C^3 Instrument Bay. A secondary factor in these results is the additional thickness of material encountered by the incident X–ray radiation at a 45 degree angle.

The results for the weapon detonation directly in front of the platform (Tables 14–17) show several orders of magnitude difference in the dose received by the components in the side of the platform closest to the detonation and the corresponding components in the side of the platform away from the detonation. Again, the differences are attributed to the shielding from within the platform architecture itself. Also, the dose received by the components in the side closest to the source were generally lower than the dose received by the same components in the detonation scenario with the source directly above the platform. This result is primarily due to the smaller cross sectional area the components present to the incident source. In some instances there was "total" shielding of particular components and "no dose" was received by these detectors. Obviously, some dose will be received by these components, but the sensitivity of the calculations is not sufficient to predict it.

In general, the dose to the sensitive components within the exterior hull of the platform was insufficient to cause any damage at a 1 cal/cm^2 exterior wall loading. At higher wall loadings, some of the KKV computers and sensors begin to receive doses sufficient enough to cause damage. Furthermore, the majority of the dose to the internal components of the SBI platform came from blackbody devices with temperatures greater than 10 keV. The low temperature devices will yield a higher flux of X–rays, but the incident energy will be insufficient to cause permanent damage to the internal electronic components. The effects of shielding from within the platform architecture is seen by the different dose levels received in the KKVs and fuel tanks. Finally, because of the low dose levels to the components within the exterior hull of the platform, no additional shielding is required. However, sensors and electronic components on the surface or outside of the exterior hull will require some form of X–ray shielding to survive the effects of a weapon detonation yielding a wall loading of 1 cal/cm^2 or greater.

Table 8

Dose (in rads-cm^2/X-Ray) to the SBI Weapon Platform for Various Temperature Blackbody X-Ray Sources Located Directly Above the SBI Platform

Detector Region	Temperature of Blackbody Source 2 keV	5 keV	10 keV	20 keV
1	0.000+00 ± 0.0	2.748−17[a] ± 45.2[b]	7.931−15 ± 26.5	6.278−14 ± 9.7
2	0.000+00 ± 0.0	2.896−17 ± 22.1	3.241−15 ± 15.8	4.246−14 ± 10.4
3	0.000+00 ± 0.0	5.503−18 ± 19.3	3.235−15 ± 33.1	3.533−14 ± 16.9
4	0.000+00 ± 0.0	2.896−17 ± 22.1	3.241−15 ± 15.8	4.246−14 ± 10.4
5	0.000+00 ± 0.0	1.374−16 ± 18.5	5.239−15 ± 9.3	6.153−14 ± 7.3
6	0.000+00 ± 0.0	9.171−17 ± 42.0	7.952−15 ± 13.8	7.949−14 ± 9.1
7	0.000+00 ± 0.0	1.374−16 ± 18.5	5.239−15 ± 9.3	6.153−14 ± 7.3
8	1.613−20 ± 58.9	1.905−16 ± 18.3	7.580−15 ± 8.9	5.886−14 ± 5.7
9	0.000+00 ± 0.0	2.702−17 ± 22.6	2.425−15 ± 16.4	1.634−14 ± 12.6
10	0.000+00 ± 0.0	2.702−17 ± 22.6	2.425−15 ± 16.4	1.634−14 ± 12.6
11	1.613−20 ± 58.9	1.905−16 ± 18.3	7.580−15 ± 8.9	5.886−14 ± 5.7
12	4.423−18 ± 16.5	4.811−15 ± 6.6	6.820−14 ± 4.0	2.639−13 ± 3.2
13	1.708−18 ± 26.2	3.248−15 ± 8.7	4.190−14 ± 4.2	2.165−13 ± 3.6
14	1.708−18 ± 26.2	3.248−15 ± 8.7	4.190−14 ± 4.2	2.165−13 ± 3.6
15	4.423−18 ± 16.5	4.811−15 ± 6.6	6.820−14 ± 4.0	2.639−13 ± 3.2
16	1.558−20 ± 49.9	2.178−16 ± 14.5	1.435−14 ± 10.9	9.569−14 ± 5.3
17	0.000+00 ± 0.0	4.966−17 ± 21.1	3.037−15 ± 15.1	2.956−14 ± 11.4
18	9.332−18 ± 13.7	1.010−14 ± 5.6	1.221−13 ± 3.9	4.131−13 ± 4.4
19	1.311−18 ± 16.1	3.880−15 ± 6.1	6.855−14 ± 4.1	2.179−13 ± 3.3
20	1.311−18 ± 16.1	3.880−15 ± 6.1	6.855−14 ± 4.1	2.179−13 ± 3.3
21	1.558−20 ± 49.9	2.178−16 ± 14.5	1.435−14 ± 10.9	9.569−14 ± 5.3
22	0.000+00 ± 0.0	4.966−17 ± 21.1	3.037−15 ± 15.1	2.956−14 ± 11.4
23	9.332−18 ± 13.7	1.010−14 ± 5.6	1.221−13 ± 3.9	4.131−13 ± 4.4
24	1.311−18 ± 16.1	3.880−15 ± 6.1	6.855−14 ± 4.1	2.179−13 ± 3.3
25	1.311−18 ± 16.1	3.880−15 ± 6.1	6.855−14 ± 4.1	2.179−13 ± 3.3
26	1.953−19 ± 99.9	9.782−17 ± 18.1	6.693−15 ± 7.4	6.989−14 ± 3.1
27	0.000+00 ± 0.0	8.261−17 ± 20.7	2.363−15 ± 13.2	2.439−14 ± 9.8
28	4.645−18 ± 12.1	7.879−15 ± 5.9	1.012−13 ± 3.6	3.553−13 ± 3.1
29	6.221−19 ± 14.7	2.496−15 ± 4.6	3.934−14 ± 2.2	1.852−13 ± 2.7
30	6.221−19 ± 14.7	2.496−15 ± 4.6	3.934−14 ± 2.2	1.852−13 ± 2.7
31	1.953−19 ± 99.9	9.782−17 ± 18.1	6.693−15 ± 7.4	6.989−14 ± 3.1
32	0.000+00 ± 0.0	8.261−17 ± 20.7	2.363−15 ± 13.2	2.439−14 ± 9.8
33	4.645−18 ± 12.1	7.879−15 ± 5.9	1.012−13 ± 3.6	3.553−13 ± 3.1
34	6.221−19 ± 14.7	2.496−15 ± 4.6	3.934−14 ± 2.2	1.852−13 ± 2.7
35	6.221−19 ± 14.7	2.496−15 ± 4.6	3.934−14 ± 2.2	1.852−13 ± 2.7

[a] Read as 2.748×10^{-17}.
[b] Percent Fractional Standard Deviation.

Table 8 - continued

Detector Region	Temperature of Blackbody Source 2 keV	5 keV	10 keV	20 keV
36	8.301−15 ± 5.9	1.748−13 ± 2.2	3.423−13 ± 5.1	4.076−13 ± 4.6
37	1.285−14 ± 5.2	1.882−13 ± 2.4	3.657−13 ± 3.3	4.469−13 ± 5.3
38	2.188−14 ± 4.0	2.171−13 ± 2.3	3.859−13 ± 3.2	4.577−13 ± 4.4
39	6.090−14 ± 3.2	3.547−13 ± 1.9	4.402−13 ± 3.8	4.854−13 ± 2.9
40	7.427−13 ± 0.5	9.185−13 ± 1.0	5.885−13 ± 2.9	5.081−13 ± 3.9
41	8.301−15 ± 5.9	1.748−13 ± 2.2	3.423−13 ± 5.1	4.076−13 ± 4.6
42	1.285−14 ± 5.2	1.882−13 ± 2.4	3.657−13 ± 3.3	4.469−13 ± 5.3
43	2.188−14 ± 4.0	2.171−13 ± 2.3	3.859−13 ± 3.2	4.577−13 ± 4.4
44	6.090−14 ± 3.2	3.547−13 ± 1.9	4.402−13 ± 3.8	4.854−13 ± 2.9
45	7.427−13 ± 0.5	9.185−13 ± 1.0	5.885−13 ± 2.9	5.081−13 ± 3.9
46	1.158−16 ± 12.7	4.398−14 ± 6.8	3.996−13 ± 4.8	7.672−13 ± 7.0
47	1.860−16 ± 11.4	7.123−14 ± 3.8	4.027−13 ± 2.7	8.217−13 ± 3.3
48	4.545−16 ± 9.1	9.451−14 ± 4.1	4.837−13 ± 4.3	8.368−13 ± 5.3
49	2.857−15 ± 6.1	2.145−13 ± 3.2	6.214−13 ± 3.3	1.048−12 ± 3.7
50	7.460−13 ± 1.6	1.554−12 ± 1.2	1.533−12 ± 1.9	1.331−12 ± 2.5
51	6.244−22 ± 84.1	1.268−16 ± 17.7	3.011−15 ± 7.4	2.976−14 ± 5.5
52	0.000+00 ± 0.0	1.582−17 ± 23.8	8.727−16 ± 12.6	1.035−14 ± 7.8
53	3.576−18 ± 13.1	3.260−15 ± 6.6	3.471−14 ± 3.4	1.443−13 ± 3.0
54	4.152−19 ± 15.2	1.130−15 ± 6.1	1.730−14 ± 3.9	8.361−14 ± 2.8
55	4.152−19 ± 15.2	1.130−15 ± 6.1	1.730−14 ± 3.9	8.361−14 ± 2.8
56	6.244−22 ± 84.1	1.268−16 ± 17.7	3.011−15 ± 7.4	2.976−14 ± 5.5
57	0.000+00 ± 0.0	1.582−17 ± 23.8	8.727−16 ± 12.6	1.035−14 ± 7.8
58	3.576−18 ± 13.1	3.260−15 ± 6.6	3.471−14 ± 3.4	1.443−13 ± 3.0
59	4.152−19 ± 15.2	1.130−15 ± 6.1	1.730−14 ± 3.9	8.361−14 ± 2.8
60	4.152−19 ± 15.2	1.130−15 ± 6.1	1.730−14 ± 3.9	8.361−14 ± 2.8
61	4.630−22 ± 35.2	4.979−17 ± 9.4	1.615−15 ± 4.0	1.419−14 ± 2.1
62	4.630−22 ± 35.2	4.979−17 ± 9.4	1.615−15 ± 4.0	1.419−14 ± 2.1
63	7.781−18 ± 5.2	4.989−15 ± 1.6	4.490−14 ± 1.3	1.608−13 ± 0.8
64	7.781−18 ± 5.2	4.989−15 ± 1.6	4.490−14 ± 1.3	1.608−13 ± 0.8
65	4.630−22 ± 35.2	4.979−17 ± 9.4	1.615−15 ± 4.0	1.419−14 ± 2.1
66	4.630−22 ± 35.2	4.979−17 ± 9.4	1.615−15 ± 4.0	1.419−14 ± 2.1
67	7.781−18 ± 5.2	4.989−15 ± 1.6	4.490−14 ± 1.3	1.608−13 ± 0.8
68	7.781−18 ± 5.2	4.989−15 ± 1.6	4.490−14 ± 1.3	1.608−13 ± 0.8

Table 9

Total Dose (in rads) due to a 2 keV Temperature Blackbody X-Ray Source Located Directly Above the SBI Weapon Platform

Detector Region	Exterior Wall Loading 1 cal/cm^2	2 cal/cm^2	5 cal/cm^2	10 cal/cm^2	% FSD
1	0.000+00	0.000+00	0.000+00	0.000+00	0.0
2	0.000+00	0.000+00	0.000+00	0.000+00	0.0
3	0.000+00	0.000+00	0.000+00	0.000+00	0.0
4	0.000+00	0.000+00	0.000+00	0.000+00	0.0
5	0.000+00	0.000+00	0.000+00	0.000+00	0.0
6	0.000+00	0.000+00	0.000+00	0.000+00	0.0
7	0.000+00	0.000+00	0.000+00	0.000+00	0.0
8	7.836−05[a]	1.567−04	3.918−04	7.836−04	58.9
9	0.000+00	0.000+00	0.000+00	0.000+00	0.0
10	0.000+00	0.000+00	0.000+00	0.000+00	0.0
11	7.836−05	1.567−04	3.918−04	7.836−04	58.9
12	2.148−02	4.297−02	1.074−01	2.148−01	16.5
13	8.294−03	1.659−02	4.147−02	8.294−02	26.2
14	8.294−03	1.659−02	4.147−02	8.294−02	26.2
15	2.148−02	4.297−02	1.074−01	2.148−01	16.5
16	7.568−05	1.514−04	3.784−04	7.568−04	49.9
17	0.000+00	0.000+00	0.000+00	0.000+00	0.0
18	4.532−02	9.065−02	2.266−01	4.532−01	13.7
19	6.367−03	1.273−02	3.183−02	6.367−02	16.1
20	6.367−03	1.273−02	3.183−02	6.367−02	16.1
21	7.568−05	1.514−04	3.784−04	7.568−04	49.9
22	0.000+00	0.000+00	0.000+00	0.000+00	0.0
23	4.532−02	9.065−02	2.266−01	4.532−01	13.7
24	6.367−03	1.273−02	3.183−02	6.367−02	16.1
25	6.367−03	1.273−02	3.183−02	6.367−02	16.1
26	9.484−04	1.897−03	4.742−03	9.484−03	99.9
27	0.000+00	0.000+00	0.000+00	0.000+00	0.0
28	2.256−02	4.512−02	1.128−01	2.256−01	12.1
29	3.021−03	6.043−03	1.511−02	3.021−02	14.7
30	3.021−03	6.043−03	1.511−02	3.021−02	14.7
31	9.484−04	1.897−03	4.742−03	9.484−03	99.9
32	0.000+00	0.000+00	0.000+00	0.000+00	0.0
33	2.256−02	4.512−02	1.128−01	2.256−01	12.1
34	3.021−03	6.043−03	1.511−02	3.021−02	14.7
35	3.021−03	6.043−03	1.511−02	3.021−02	14.7

[a]Read as 7.836×10^{-5}.

Table 9 - continued

Detector Region	Exterior Wall Loading 1 cal/cm^2	2 cal/cm^2	5 cal/cm^2	10 cal/cm^2	% FSD
36	4.032+01	8.064+01	2.016+02	4.032+02	5.9
37	6.243+01	1.249+02	3.122+02	6.243+02	5.2
38	1.063+02	2.126+02	5.314+02	1.063+03	4.0
39	2.958+02	5.916+02	1.479+03	2.958+03	3.2
40	3.608+03	7.215+03	1.804+04	3.608+04	0.5
41	4.032+01	8.064+01	2.016+02	4.032+02	5.9
42	6.243+01	1.249+02	3.122+02	6.243+02	5.2
43	1.063+02	2.126+02	5.314+02	1.063+03	4.0
44	2.958+02	5.916+02	1.479+03	2.958+03	3.2
45	3.608+03	7.215+03	1.804+04	3.608+04	0.5
46	5.626−01	1.125+00	2.813+00	5.626+00	12.7
47	9.036−01	1.807+00	4.518+00	9.036+00	11.4
48	2.207+00	4.415+00	1.104+01	2.207+01	9.1
49	1.388+01	2.776+01	6.939+01	1.388+02	6.1
50	3.623+03	7.246+03	1.812+04	3.623+04	1.6
51	3.033−06	6.066−06	1.516−05	3.033−05	84.1
52	0.000+00	0.000+00	0.000+00	0.000+00	0.0
53	1.737−02	3.473−02	8.684−02	1.737−01	13.1
54	2.017−03	4.033−03	1.008−02	2.017−02	15.2
55	2.017−03	4.033−03	1.008−02	2.017−02	15.2
56	3.033−06	6.066−06	1.516−05	3.033−05	84.1
57	0.000+00	0.000+00	0.000+00	0.000+00	0.0
58	1.737−02	3.473−02	8.684−02	1.737−01	13.1
59	2.017−03	4.033−03	1.008−02	2.017−02	15.2
60	2.017−03	4.033−03	1.008−02	2.017−02	15.2
61	2.249−06	4.498−06	1.124−05	2.249−05	35.2
62	2.249−06	4.498−06	1.124−05	2.249−05	35.2
63	3.779−02	7.559−02	1.890−01	3.779−01	5.2
64	3.779−02	7.559−02	1.890−01	3.779−01	5.2
65	2.249−06	4.498−06	1.124−05	2.249−05	35.2
66	2.249−06	4.498−06	1.124−05	2.249−05	35.2
67	3.779−02	7.559−02	1.890−01	3.779−01	5.2
68	3.779−02	7.559−02	1.890−01	3.779−01	5.2

Table 10

Total Dose (in rads) due to a 5 keV Temperature Blackbody X-Ray Source Located Directly Above the SBI Weapon Platform

Detector	Exterior Wall Loading				
Region	1 cal/cm^2	2 cal/cm^2	5 cal/cm^2	10 cal/cm^2	% FSD
1	5.318−02[a]	1.064−01	2.659−01	5.318−01	45.2
2	5.604−02	1.121−01	2.802−01	5.604−01	22.1
3	1.065−02	2.130−02	5.325−02	1.065−01	19.3
4	5.604−02	1.121−01	2.802−01	5.604−01	22.1
5	2.659−01	5.318−01	1.329+00	2.659+00	18.5
6	1.775−01	3.550−01	8.874−01	1.775+00	42.0
7	2.659−01	5.318−01	1.329+00	2.659+00	18.5
8	3.686−01	7.372−01	1.843+00	3.686+00	18.3
9	5.228−02	1.046−01	2.614−01	5.228−01	22.6
10	5.228−02	1.046−01	2.614−01	5.228−01	22.6
11	3.686−01	7.372−01	1.843+00	3.686+00	18.3
12	9.310+00	1.862+01	4.655+01	9.310+01	6.6
13	6.285+00	1.257+01	3.143+01	6.285+01	8.7
14	6.285+00	1.257+01	3.143+01	6.285+01	8.7
15	9.310+00	1.862+01	4.655+01	9.310+01	6.6
16	4.215−01	8.430−01	2.107+00	4.215+00	14.5
17	9.611−02	1.922−01	4.806−01	9.611−01	21.1
18	1.955+01	3.910+01	9.774+01	1.955+02	5.6
19	7.508+00	1.502+01	3.754+01	7.508+01	6.1
20	7.508+00	1.502+01	3.754+01	7.508+01	6.1
21	4.215−01	8.430−01	2.107+00	4.215+00	14.5
22	9.611−02	1.922−01	4.806−01	9.611−01	21.1
23	1.955+01	3.910+01	9.774+01	1.955+02	5.6
24	7.508+00	1.502+01	3.754+01	7.508+01	6.1
25	7.508+00	1.502+01	3.754+01	7.508+01	6.1
26	1.893−01	3.786−01	9.465−01	1.893+00	18.1
27	1.599−01	3.197−01	7.994−01	1.599+00	20.7
28	1.525+01	3.050+01	7.624+01	1.525+02	5.9
29	4.830+00	9.660+00	2.415+01	4.830+01	4.6
30	4.830+00	9.660+00	2.415+01	4.830+01	4.6
31	1.893−01	3.786−01	9.465−01	1.893+00	18.1
32	1.599−01	3.197−01	7.994−01	1.599+00	20.7
33	1.525+01	3.050+01	7.624+01	1.525+02	5.9
34	4.830+00	9.660+00	2.415+01	4.830+01	4.6
35	4.830+00	9.660+00	2.415+01	4.830+01	4.6

[a]Read as 5.318×10^{-2}.

Table 10 - continued

Detector Region	Exterior Wall Loading 1 cal/cm^2	2 cal/cm^2	5 cal/cm^2	10 cal/cm^2	% FSD
36	3.383+02	6.765+02	1.691+03	3.383+03	2.2
37	3.642+02	7.284+02	1.821+03	3.642+03	2.4
38	4.202+02	8.404+02	2.101+03	4.202+03	2.3
39	6.865+02	1.373+03	3.432+03	6.865+03	1.9
40	1.778+03	3.555+03	8.888+03	1.778+04	1.0
41	3.383+02	6.765+02	1.691+03	3.383+03	2.2
42	3.642+02	7.284+02	1.821+03	3.642+03	2.4
43	4.202+02	8.404+02	2.101+03	4.202+03	2.3
44	6.865+02	1.373+03	3.432+03	6.865+03	1.9
45	1.778+03	3.555+03	8.888+03	1.778+04	1.0
46	8.511+01	1.702+02	4.255+02	8.511+02	6.8
47	1.378+02	2.757+02	6.892+02	1.378+03	3.8
48	1.829+02	3.658+02	9.145+02	1.829+03	4.1
49	4.150+02	8.300+02	2.075+03	4.150+03	3.2
50	3.007+03	6.014+03	1.504+04	3.007+04	1.2
51	2.453−01	4.906−01	1.227+00	2.453+00	17.7
52	3.061−02	6.122−02	1.530−01	3.061−01	23.8
53	6.308+00	1.262+01	3.154+01	6.308+01	6.6
54	2.187+00	4.375+00	1.094+01	2.187+01	6.1
55	2.187+00	4.375+00	1.094+01	2.187+01	6.1
56	2.453−01	4.906−01	1.227+00	2.453+00	17.7
57	3.061−02	6.122−02	1.530−01	3.061−01	23.8
58	6.308+00	1.262+01	3.154+01	6.308+01	6.6
59	2.187+00	4.375+00	1.094+01	2.187+01	6.1
60	2.187+00	4.375+00	1.094+01	2.187+01	6.1
61	9.636−02	1.927−01	4.818−01	9.636−01	9.4
62	9.636−02	1.927−01	4.818−01	9.636−01	9.4
63	9.655+00	1.931+01	4.827+01	9.655+01	1.6
64	9.655+00	1.931+01	4.827+01	9.655+01	1.6
65	9.636−02	1.927−01	4.818−01	9.636−01	9.4
66	9.636−02	1.927−01	4.818−01	9.636−01	9.4
67	9.655+00	1.931+01	4.827+01	9.655+01	1.6
68	9.655+00	1.931+01	4.827+01	9.655+01	1.6

Table 11

Total Dose (in rads) due to a 10 keV Temperature Blackbody X-Ray Source Located Directly Above the SBI Weapon Platform

Detector Region	Exterior Wall Loading 1 cal/cm^2	2 cal/cm^2	5 cal/cm^2	10 cal/cm^2	% FSD
1	7.671+00[a]	1.534+01	3.835+01	7.671+01	26.5
2	3.135+00	6.269+00	1.567+01	3.135+01	15.8
3	3.129+00	6.258+00	1.565+01	3.129+01	33.1
4	3.135+00	6.269+00	1.567+01	3.135+01	15.8
5	5.067+00	1.013+01	2.534+01	5.067+01	9.3
6	7.692+00	1.538+01	3.846+01	7.692+01	13.8
7	5.067+00	1.013+01	2.534+01	5.067+01	9.3
8	7.332+00	1.466+01	3.666+01	7.332+01	8.9
9	2.346+00	4.692+00	1.173+01	2.346+01	16.4
10	2.346+00	4.692+00	1.173+01	2.346+01	16.4
11	7.332+00	1.466+01	3.666+01	7.332+01	8.9
12	6.596+01	1.319+02	3.298+02	6.596+02	4.0
13	4.053+01	8.107+01	2.027+02	4.053+02	4.2
14	4.053+01	8.107+01	2.027+02	4.053+02	4.2
15	6.596+01	1.319+02	3.298+02	6.596+02	4.0
16	1.388+01	2.776+01	6.940+01	1.388+02	10.9
17	2.938+00	5.875+00	1.469+01	2.938+01	15.1
18	1.181+02	2.363+02	5.907+02	1.181+03	3.9
19	6.630+01	1.326+02	3.315+02	6.630+02	4.1
20	6.630+01	1.326+02	3.315+02	6.630+02	4.1
21	1.388+01	2.776+01	6.940+01	1.388+02	10.9
22	2.938+00	5.875+00	1.469+01	2.938+01	15.1
23	1.181+02	2.363+02	5.907+02	1.181+03	3.9
24	6.630+01	1.326+02	3.315+02	6.630+02	4.1
25	6.630+01	1.326+02	3.315+02	6.630+02	4.1
26	6.474+00	1.295+01	3.237+01	6.474+01	7.4
27	2.285+00	4.571+00	1.143+01	2.285+01	13.2
28	9.784+01	1.957+02	4.892+02	9.784+02	3.6
29	3.806+01	7.611+01	1.903+02	3.806+02	2.2
30	3.806+01	7.611+01	1.903+02	3.806+02	2.2
31	6.474+00	1.295+01	3.237+01	6.474+01	7.4
32	2.285+00	4.571+00	1.143+01	2.285+01	13.2
33	9.784+01	1.957+02	4.892+02	9.784+02	3.6
34	3.806+01	7.611+01	1.903+02	3.806+02	2.2
35	3.806+01	7.611+01	1.903+02	3.806+02	2.2

[a]Read as 7.671×10^0.

Table 11 - continued

Detector Region	Exterior Wall Loading 1 cal/cm^2	2 cal/cm^2	5 cal/cm^2	10 cal/cm^2	% FSD
36	3.311+02	6.621+02	1.655+03	3.311+03	5.1
37	3.538+02	7.075+02	1.769+03	3.538+03	3.3
38	3.733+02	7.466+02	1.866+03	3.733+03	3.2
39	4.258+02	8.515+02	2.129+03	4.258+03	3.8
40	5.692+02	1.138+03	2.846+03	5.692+03	2.9
41	3.311+02	6.621+02	1.655+03	3.311+03	5.1
42	3.538+02	7.075+02	1.769+03	3.538+03	3.3
43	3.733+02	7.466+02	1.866+03	3.733+03	3.2
44	4.258+02	8.515+02	2.129+03	4.258+03	3.8
45	5.692+02	1.138+03	2.846+03	5.692+03	2.9
46	3.865+02	7.731+02	1.933+03	3.865+03	4.8
47	3.895+02	7.791+02	1.948+03	3.895+03	2.7
48	4.679+02	9.357+02	2.339+03	4.679+03	4.3
49	6.011+02	1.202+03	3.005+03	6.011+03	3.3
50	1.483+03	2.965+03	7.413+03	1.483+04	1.9
51	2.913+00	5.825+00	1.456+01	2.913+01	7.4
52	8.441−01	1.688+00	4.221+00	8.441+00	12.6
53	3.357+01	6.714+01	1.679+02	3.357+02	3.4
54	1.673+01	3.347+01	8.367+01	1.673+02	3.9
55	1.673+01	3.347+01	8.367+01	1.673+02	3.9
56	2.913+00	5.825+00	1.456+01	2.913+01	7.4
57	8.441−01	1.688+00	4.221+00	8.441+00	12.6
58	3.357+01	6.714+01	1.679+02	3.357+02	3.4
59	1.673+01	3.347+01	8.367+01	1.673+02	3.9
60	1.673+01	3.347+01	8.367+01	1.673+02	3.9
61	1.562+00	3.123+00	7.808+00	1.562+01	4.0
62	1.562+00	3.123+00	7.808+00	1.562+01	4.0
63	4.343+01	8.686+01	2.171+02	4.343+02	1.3
64	4.343+01	8.686+01	2.171+02	4.343+02	1.3
65	1.562+00	3.123+00	7.808+00	1.562+01	4.0
66	1.562+00	3.123+00	7.808+00	1.562+01	4.0
67	4.343+01	8.686+01	2.171+02	4.343+02	1.3
68	4.343+01	8.686+01	2.171+02	4.343+02	1.3

Table 12

Total Dose (in rads) due to a 20 keV Temperature Blackbody X-Ray Source Located Directly Above the SBI Weapon Platform

Detector	Exterior Wall Loading				
Region	1 cal/cm^2	2 cal/cm^2	5 cal/cm^2	10 cal/cm^2	% FSD
1	3.036+01[a]	6.072+01	1.518+02	3.036+02	9.7
2	2.053+01	4.107+01	1.027+02	2.053+02	10.4
3	1.709+01	3.417+01	8.543+01	1.709+02	16.9
4	2.053+01	4.107+01	1.027+02	2.053+02	10.4
5	2.976+01	5.952+01	1.488+02	2.976+02	7.3
6	3.844+01	7.689+01	1.922+02	3.844+02	9.1
7	2.976+01	5.952+01	1.488+02	2.976+02	7.3
8	2.847+01	5.694+01	1.423+02	2.847+02	5.7
9	7.901+00	1.580+01	3.951+01	7.901+01	12.6
10	7.901+00	1.580+01	3.951+01	7.901+01	12.6
11	2.847+01	5.694+01	1.423+02	2.847+02	5.7
12	1.276+02	2.553+02	6.381+02	1.276+03	3.2
13	1.047+02	2.094+02	5.235+02	1.047+03	3.6
14	1.047+02	2.094+02	5.235+02	1.047+03	3.6
15	1.276+02	2.553+02	6.381+02	1.276+03	3.2
16	4.628+01	9.256+01	2.314+02	4.628+02	5.3
17	1.429+01	2.859+01	7.147+01	1.429+02	11.4
18	1.998+02	3.996+02	9.989+02	1.998+03	4.4
19	1.054+02	2.108+02	5.269+02	1.054+03	3.3
20	1.054+02	2.108+02	5.269+02	1.054+03	3.3
21	4.628+01	9.256+01	2.314+02	4.628+02	5.3
22	1.429+01	2.859+01	7.147+01	1.429+02	11.4
23	1.998+02	3.996+02	9.989+02	1.998+03	4.4
24	1.054+02	2.108+02	5.269+02	1.054+03	3.3
25	1.054+02	2.108+02	5.269+02	1.054+03	3.3
26	3.380+01	6.760+01	1.690+02	3.380+02	3.1
27	1.180+01	2.359+01	5.898+01	1.180+02	9.8
28	1.718+02	3.437+02	8.591+02	1.718+03	3.1
29	8.958+01	1.792+02	4.479+02	8.958+02	2.7
30	8.958+01	1.792+02	4.479+02	8.958+02	2.7
31	3.380+01	6.760+01	1.690+02	3.380+02	3.1
32	1.180+01	2.359+01	5.898+01	1.180+02	9.8
33	1.718+02	3.437+02	8.591+02	1.718+03	3.1
34	8.958+01	1.792+02	4.479+02	8.958+02	2.7
35	8.958+01	1.792+02	4.479+02	8.958+02	2.7

[a]Read as 3.036×10^1.

Table 12 - continued

Detector Region	Exterior Wall Loading 1 cal/cm^2	2 cal/cm^2	5 cal/cm^2	10 cal/cm^2	% FSD
36	1.971+02	3.942+02	9.856+02	1.971+03	4.6
37	2.161+02	4.323+02	1.081+03	2.161+03	5.3
38	2.214+02	4.428+02	1.107+03	2.214+03	4.4
39	2.347+02	4.695+02	1.174+03	2.347+03	2.9
40	2.457+02	4.915+02	1.229+03	2.457+03	3.9
41	1.971+02	3.942+02	9.856+02	1.971+03	4.6
42	2.161+02	4.323+02	1.081+03	2.161+03	5.3
43	2.214+02	4.428+02	1.107+03	2.214+03	4.4
44	2.347+02	4.695+02	1.174+03	2.347+03	2.9
45	2.457+02	4.915+02	1.229+03	2.457+03	3.9
46	3.711+02	7.421+02	1.855+03	3.711+03	7.0
47	3.974+02	7.948+02	1.987+03	3.974+03	3.3
48	4.047+02	8.095+02	2.024+03	4.047+03	5.3
49	5.068+02	1.014+03	2.534+03	5.068+03	3.7
50	6.437+02	1.287+03	3.218+03	6.437+03	2.5
51	1.439+01	2.879+01	7.196+01	1.439+02	5.5
52	5.008+00	1.002+01	2.504+01	5.008+01	7.8
53	6.977+01	1.395+02	3.489+02	6.977+02	3.0
54	4.044+01	8.087+01	2.022+02	4.044+02	2.8
55	4.044+01	8.087+01	2.022+02	4.044+02	2.8
56	1.439+01	2.879+01	7.196+01	1.439+02	5.5
57	5.008+00	1.002+01	2.504+01	5.008+01	7.8
58	6.977+01	1.395+02	3.489+02	6.977+02	3.0
59	4.044+01	8.087+01	2.022+02	4.044+02	2.8
60	4.044+01	8.087+01	2.022+02	4.044+02	2.8
61	6.863+00	1.373+01	3.431+01	6.863+01	2.1
62	6.863+00	1.373+01	3.431+01	6.863+01	2.1
63	7.778+01	1.556+02	3.889+02	7.778+02	0.8
64	7.778+01	1.556+02	3.889+02	7.778+02	0.8
65	6.863+00	1.373+01	3.431+01	6.863+01	2.1
66	6.863+00	1.373+01	3.431+01	6.863+01	2.1
67	7.778+01	1.556+02	3.889+02	7.778+02	0.8
68	7.778+01	1.556+02	3.889+02	7.778+02	0.8

Table 13

Dose (in rads-cm^2/X-Ray) to the SBI Weapon Platform for Various Temperature Blackbody X-Ray Sources Located Directly in Front of the SBI Platform

Detector Region	Temperature of Blackbody Source 2 keV	5 keV	10 keV	20 keV
1	1.541−20[a] ± 67.6[b]	1.221−16 ± 16.6	4.267−15 ± 16.7	3.688−14 ± 10.7
2	1.175−17 ± 7.0	8.693−15 ± 2.7	7.825−14 ± 2.0	2.245−13 ± 1.4
3	1.779−17 ± 12.1	7.632−15 ± 4.4	6.833−14 ± 3.0	2.030−13 ± 3.3
4	1.175−17 ± 7.0	8.693−15 ± 2.7	7.825−14 ± 2.0	2.245−13 ± 1.4
5	1.175−17 ± 7.0	8.693−15 ± 2.7	7.825−14 ± 2.0	2.245−13 ± 1.4
6	1.779−17 ± 12.1	7.632−15 ± 4.4	6.833−14 ± 3.0	2.030−13 ± 3.3
7	1.175−17 ± 7.0	8.693−15 ± 2.7	7.825−14 ± 2.0	2.245−13 ± 1.4
8	3.321−18 ± 7.0	2.443−15 ± 2.7	2.645−14 ± 2.0	8.532−14 ± 1.6
9	3.321−18 ± 7.0	2.443−15 ± 2.7	2.645−14 ± 2.0	8.532−14 ± 1.6
10	3.321−18 ± 7.0	2.443−15 ± 2.7	2.645−14 ± 2.0	8.532−14 ± 1.6
11	3.321−18 ± 7.0	2.443−15 ± 2.7	2.645−14 ± 2.0	8.532−14 ± 1.6
12	3.321−18 ± 7.0	2.443−15 ± 2.7	2.645−14 ± 2.0	8.532−14 ± 1.6
13	3.321−18 ± 7.0	2.443−15 ± 2.7	2.645−14 ± 2.0	8.532−14 ± 1.6
14	3.321−18 ± 7.0	2.443−15 ± 2.7	2.645−14 ± 2.0	8.532−14 ± 1.6
15	3.321−18 ± 7.0	2.443−15 ± 2.7	2.645−14 ± 2.0	8.532−14 ± 1.6
16	4.611−20 ± 53.0	4.148−16 ± 19.4	5.792−15 ± 11.3	5.714−14 ± 7.0
17	1.148−21 ± 56.3	1.899−16 ± 9.3	6.350−15 ± 5.3	4.252−14 ± 3.7
18	1.148−21 ± 56.3	1.899−16 ± 9.3	6.350−15 ± 5.3	4.252−14 ± 3.7
19	1.148−21 ± 56.3	1.899−16 ± 9.3	6.350−15 ± 5.3	4.252−14 ± 3.7
20	1.148−21 ± 56.3	1.899−16 ± 9.3	6.350−15 ± 5.3	4.252−14 ± 3.7
21	0.000+00 ± 0.0	7.675−20 ± 65.9	1.985−17 ± 30.6	1.472−16 ± 26.3
22	0.000+00 ± 0.0	9.646−21 ± 44.0	2.930−18 ± 36.8	1.746−16 ± 29.4
23	0.000+00 ± 0.0	9.646−21 ± 44.0	2.930−18 ± 36.8	1.746−16 ± 29.4
24	0.000+00 ± 0.0	9.646−21 ± 44.0	2.930−18 ± 36.8	1.746−16 ± 29.4
25	0.000+00 ± 0.0	9.646−21 ± 44.0	2.930−18 ± 36.8	1.746−16 ± 29.4
26	6.346−18 ± 11.6	5.594−15 ± 5.1	6.394−14 ± 3.9	2.376−13 ± 3.0
27	4.444−18 ± 6.1	5.272−15 ± 2.2	6.499−14 ± 1.1	2.156−13 ± 1.4
28	4.444−18 ± 6.1	5.272−15 ± 2.2	6.499−14 ± 1.1	2.156−13 ± 1.4
29	4.444−18 ± 6.1	5.272−15 ± 2.2	6.499−14 ± 1.1	2.156−13 ± 1.4
30	4.444−18 ± 6.1	5.272−15 ± 2.2	6.499−14 ± 1.1	2.156−13 ± 1.4
31	0.000+00 ± 0.0	1.298−20 ± 70.6	1.831−16 ± 33.3	2.006−15 ± 31.8
32	0.000+00 ± 0.0	2.025−20 ± 44.8	9.528−17 ± 18.6	6.844−16 ± 18.3
33	0.000+00 ± 0.0	2.025−20 ± 44.8	9.528−17 ± 18.6	6.844−16 ± 18.3
34	0.000+00 ± 0.0	2.025−20 ± 44.8	9.528−17 ± 18.6	6.844−16 ± 18.3
35	0.000+00 ± 0.0	2.025−20 ± 44.8	9.528−17 ± 18.6	6.844−16 ± 18.3

[a] Read as 1.541×10^{-20}.
[b] Percent Fractional Standard Deviation.

Table 13 - continued

Detector Region	2 keV	Temperature of Blackbody Source 5 keV	10 keV	20 keV
36	5.539−23 ± 66.0	3.314−18 ± 21.5	8.381−17 ± 14.4	2.945−16 ± 8.6
37	1.338−22 ± 62.4	6.763−18 ± 31.5	5.093−17 ± 17.7	3.682−16 ± 9.5
38	3.406−22 ± 75.5	2.701−18 ± 32.5	7.941−17 ± 18.5	3.447−16 ± 9.5
39	7.229−23 ± 51.7	1.216−18 ± 26.7	4.453−17 ± 13.5	3.994−16 ± 8.3
40	9.190−22 ± 52.0	3.296−18 ± 24.6	1.575−16 ± 16.2	4.898−16 ± 7.9
41	5.539−23 ± 66.0	3.314−18 ± 21.5	8.381−17 ± 14.4	2.945−16 ± 8.6
42	1.338−22 ± 62.4	6.763−18 ± 31.5	5.093−17 ± 17.7	3.682−16 ± 9.5
43	3.406−22 ± 75.5	2.701−18 ± 32.5	7.941−17 ± 18.5	3.447−16 ± 9.5
44	7.229−23 ± 51.7	1.216−18 ± 26.7	4.453−17 ± 13.5	3.994−16 ± 8.3
45	9.190−22 ± 52.0	3.296−18 ± 24.6	1.575−16 ± 16.2	4.898−16 ± 7.9
46	0.000+00 ± 0.0	7.720−18 ± 42.6	5.789−16 ± 38.2	1.424−15 ± 19.5
47	0.000+00 ± 0.0	4.846−18 ± 50.0	4.320−16 ± 51.9	6.343−15 ± 24.1
48	0.000+00 ± 0.0	6.168−18 ± 35.0	1.480−16 ± 30.9	9.239−16 ± 36.5
49	0.000+00 ± 0.0	6.224−17 ± 40.5	7.810−16 ± 32.3	5.848−15 ± 22.1
50	7.680−20 ± 50.5	3.564−17 ± 26.4	1.963−15 ± 24.6	1.329−15 ± 26.6
51	3.332−20 ± 33.8	2.400−16 ± 15.6	5.679−15 ± 9.5	2.860−14 ± 4.7
52	5.809−20 ± 16.7	3.181−16 ± 6.1	4.744−15 ± 3.4	2.577−14 ± 2.4
53	5.809−20 ± 16.7	3.181−16 ± 6.1	4.744−15 ± 3.4	2.577−14 ± 2.4
54	5.809−20 ± 16.7	3.181−16 ± 6.1	4.744−15 ± 3.4	2.577−14 ± 2.4
55	5.809−20 ± 16.7	3.181−16 ± 6.1	4.744−15 ± 3.4	2.577−14 ± 2.4
56	2.946−21 ± 70.7	6.898−19 ± 43.0	1.260−16 ± 24.8	2.098−15 ± 15.6
57	0.000+00 ± 0.0	1.854−19 ± 20.6	4.317−17 ± 10.1	9.399−16 ± 8.8
58	0.000+00 ± 0.0	1.854−19 ± 20.6	4.317−17 ± 10.1	9.399−16 ± 8.8
59	0.000+00 ± 0.0	1.854−19 ± 20.6	4.317−17 ± 10.1	9.399−16 ± 8.8
60	0.000+00 ± 0.0	1.854−19 ± 20.6	4.317−17 ± 10.1	9.399−16 ± 8.8
61	6.494−18 ± 6.0	1.120−15 ± 2.5	7.207−15 ± 1.9	2.125−14 ± 1.3
62	6.494−18 ± 6.0	1.120−15 ± 2.5	7.207−15 ± 1.9	2.125−14 ± 1.3
63	6.494−18 ± 6.0	1.120−15 ± 2.5	7.207−15 ± 1.9	2.125−14 ± 1.3
64	6.494−18 ± 6.0	1.120−15 ± 2.5	7.207−15 ± 1.9	2.125−14 ± 1.3
65	4.767−22 ± 33.0	8.842−18 ± 13.0	2.114−16 ± 7.3	1.721−15 ± 3.9
66	4.767−22 ± 33.0	8.842−18 ± 13.0	2.114−16 ± 7.3	1.721−15 ± 3.9
67	4.767−22 ± 33.0	8.842−18 ± 13.0	2.114−16 ± 7.3	1.721−15 ± 3.9
68	4.767−22 ± 33.0	8.842−18 ± 13.0	2.114−16 ± 7.3	1.721−15 ± 3.9

Table 14

Total Dose (in rads) due to a 2 keV Temperature Blackbody X-Ray Source Located Directly in Front of the SBI Weapon Platform

Detector	Exterior Wall Loading				
Region	1 cal/cm^2	2 cal/cm^2	5 cal/cm^2	10 cal/cm^2	% FSD
1	7.485−05[a]	1.497−04	3.742−04	7.485−04	67.6
2	5.707−02	1.141−01	2.853−01	5.707−01	7.0
3	8.640−02	1.728−01	4.320−01	8.640−01	12.1
4	5.707−02	1.141−01	2.853−01	5.707−01	7.0
5	5.707−02	1.141−01	2.853−01	5.707−01	7.0
6	8.640−02	1.728−01	4.320−01	8.640−01	12.1
7	5.707−02	1.141−01	2.853−01	5.707−01	7.0
8	1.613−02	3.226−02	8.066−02	1.613−01	7.0
9	1.613−02	3.226−02	8.066−02	1.613−01	7.0
10	1.613−02	3.226−02	8.066−02	1.613−01	7.0
11	1.613−02	3.226−02	8.066−02	1.613−01	7.0
12	1.613−02	3.226−02	8.066−02	1.613−01	7.0
13	1.613−02	3.226−02	8.066−02	1.613−01	7.0
14	1.613−02	3.226−02	8.066−02	1.613−01	7.0
15	1.613−02	3.226−02	8.066−02	1.613−01	7.0
16	2.240−04	4.479−04	1.120−03	2.240−03	53.0
17	5.577−06	1.115−05	2.788−05	5.577−05	56.3
18	5.577−06	1.115−05	2.788−05	5.577−05	56.3
19	5.577−06	1.115−05	2.788−05	5.577−05	56.3
20	5.577−06	1.115−05	2.788−05	5.577−05	56.3
21	0.000+00	0.000+00	0.000+00	0.000+00	0.0
22	0.000+00	0.000+00	0.000+00	0.000+00	0.0
23	0.000+00	0.000+00	0.000+00	0.000+00	0.0
24	0.000+00	0.000+00	0.000+00	0.000+00	0.0
25	0.000+00	0.000+00	0.000+00	0.000+00	0.0
26	3.083−02	6.165−02	1.541−01	3.083−01	11.6
27	2.159−02	4.317−02	1.079−01	2.159−01	6.1
28	2.159−02	4.317−02	1.079−01	2.159−01	6.1
29	2.159−02	4.317−02	1.079−01	2.159−01	6.1
30	2.159−02	4.317−02	1.079−01	2.159−01	6.1
31	0.000+00	0.000+00	0.000+00	0.000+00	0.0
32	0.000+00	0.000+00	0.000+00	0.000+00	0.0
33	0.000+00	0.000+00	0.000+00	0.000+00	0.0
34	0.000+00	0.000+00	0.000+00	0.000+00	0.0
35	0.000+00	0.000+00	0.000+00	0.000+00	0.0

[a]Read as 7.485×10^{-5}.

Table 14 - continued

Detector Region	Exterior Wall Loading 1 cal/cm^2	2 cal/cm^2	5 cal/cm^2	10 cal/cm^2	% FSD
36	2.690−07	5.380−07	1.345−06	2.690−06	66.0
37	6.499−07	1.300−06	3.250−06	6.499−06	62.4
38	1.654−06	3.309−06	8.272−06	1.654−05	75.5
39	3.511−07	7.022−07	1.755−06	3.511−06	51.7
40	4.463−06	8.927−06	2.232−05	4.463−05	52.0
41	2.690−07	5.380−07	1.345−06	2.690−06	66.0
42	6.499−07	1.300−06	3.250−06	6.499−06	62.4
43	1.654−06	3.309−06	8.272−06	1.654−05	75.5
44	3.511−07	7.022−07	1.755−06	3.511−06	51.7
45	4.463−06	8.927−06	2.232−05	4.463−05	52.0
46	0.000+00	0.000+00	0.000+00	0.000+00	0.0
47	0.000+00	0.000+00	0.000+00	0.000+00	0.0
48	0.000+00	0.000+00	0.000+00	0.000+00	0.0
49	0.000+00	0.000+00	0.000+00	0.000+00	0.0
50	3.730−04	7.460−04	1.865−03	3.730−03	50.5
51	1.618−04	3.237−04	8.092−04	1.618−03	33.8
52	2.822−04	5.643−04	1.411−03	2.822−03	16.7
53	2.822−04	5.643−04	1.411−03	2.822−03	16.7
54	2.822−04	5.643−04	1.411−03	2.822−03	16.7
55	2.822−04	5.643−04	1.411−03	2.822−03	16.7
56	1.431−05	2.862−05	7.155−05	1.431−04	70.7
57	0.000+00	0.000+00	0.000+00	0.000+00	0.0
58	0.000+00	0.000+00	0.000+00	0.000+00	0.0
59	0.000+00	0.000+00	0.000+00	0.000+00	0.0
60	0.000+00	0.000+00	0.000+00	0.000+00	0.0
61	3.154−02	6.308−02	1.577−01	3.154−01	6.0
62	3.154−02	6.308−02	1.577−01	3.154−01	6.0
63	3.154−02	6.308−02	1.577−01	3.154−01	6.0
64	3.154−02	6.308−02	1.577−01	3.154−01	6.0
65	2.315−06	4.630−06	1.158−05	2.315−05	33.0
66	2.315−06	4.630−06	1.158−05	2.315−05	33.0
67	2.315−06	4.630−06	1.158−05	2.315−05	33.0
68	2.315−06	4.630−06	1.158−05	2.315−05	33.0

Table 15

Total Dose (in rads) due to a 5 keV Temperature Blackbody X-Ray Source Located Directly in Front of the SBI Weapon Platform

Detector Region	Exterior Wall Loading 1 cal/cm^2	2 cal/cm^2	5 cal/cm^2	10 cal/cm^2	% FSD
1	2.363−01[a]	4.726−01	1.181+00	2.363+00	16.6
2	1.682+01	3.365+01	8.412+01	1.682+02	2.7
3	1.477+01	2.954+01	7.385+01	1.477+02	4.4
4	1.682+01	3.365+01	8.412+01	1.682+02	2.7
5	1.682+01	3.365+01	8.412+01	1.682+02	2.7
6	1.477+01	2.954+01	7.385+01	1.477+02	4.4
7	1.682+01	3.365+01	8.412+01	1.682+02	2.7
8	4.728+00	9.456+00	2.364+01	4.728+01	2.7
9	4.728+00	9.456+00	2.364+01	4.728+01	2.7
10	4.728+00	9.456+00	2.364+01	4.728+01	2.7
11	4.728+00	9.456+00	2.364+01	4.728+01	2.7
12	4.728+00	9.456+00	2.364+01	4.728+01	2.7
13	4.728+00	9.456+00	2.364+01	4.728+01	2.7
14	4.728+00	9.456+00	2.364+01	4.728+01	2.7
15	4.728+00	9.456+00	2.364+01	4.728+01	2.7
16	8.027−01	1.605+00	4.014+00	8.027+00	19.4
17	3.675−01	7.351−01	1.838+00	3.675+00	9.3
18	3.675−01	7.351−01	1.838+00	3.675+00	9.3
19	3.675−01	7.351−01	1.838+00	3.675+00	9.3
20	3.675−01	7.351−01	1.838+00	3.675+00	9.3
21	1.485−04	2.971−04	7.426−04	1.485−03	65.9
22	1.867−05	3.734−05	9.334−05	1.867−04	44.0
23	1.867−05	3.734−05	9.334−05	1.867−04	44.0
24	1.867−05	3.734−05	9.334−05	1.867−04	44.0
25	1.867−05	3.734−05	9.334−05	1.867−04	44.0
26	1.083+01	2.165+01	5.413+01	1.083+02	5.1
27	1.020+01	2.040+01	5.101+01	1.020+02	2.2
28	1.020+01	2.040+01	5.101+01	1.020+02	2.2
29	1.020+01	2.040+01	5.101+01	1.020+02	2.2
30	1.020+01	2.040+01	5.101+01	1.020+02	2.2
31	2.513−05	5.026−05	1.256−04	2.513−04	70.6
32	3.919−05	7.837−05	1.959−04	3.919−04	44.8
33	3.919−05	7.837−05	1.959−04	3.919−04	44.8
34	3.919−05	7.837−05	1.959−04	3.919−04	44.8
35	3.919−05	7.837−05	1.959−04	3.919−04	44.8

[a]Read as 2.363×10^{-1}.

Table 15 - continued

Detector Region	Exterior Wall Loading 1 cal/cm^2	2 cal/cm^2	5 cal/cm^2	10 cal/cm^2	% FSD
36	6.414−03	1.283−02	3.207−02	6.414−02	21.5
37	1.309−02	2.617−02	6.544−02	1.309−01	31.5
38	5.228−03	1.046−02	2.614−02	5.228−02	32.5
39	2.354−03	4.708−03	1.177−02	2.354−02	26.7
40	6.379−03	1.276−02	3.190−02	6.379−02	24.6
41	6.414−03	1.283−02	3.207−02	6.414−02	21.5
42	1.309−02	2.617−02	6.544−02	1.309−01	31.5
43	5.228−03	1.046−02	2.614−02	5.228−02	32.5
44	2.354−03	4.708−03	1.177−02	2.354−02	26.7
45	6.379−03	1.276−02	3.190−02	6.379−02	24.6
46	1.494−02	2.988−02	7.470−02	1.494−01	42.6
47	9.379−03	1.876−02	4.689−02	9.379−02	50.0
48	1.194−02	2.387−02	5.968−02	1.194−01	35.0
49	1.205−01	2.409−01	6.023−01	1.205+00	40.5
50	6.897−02	1.379−01	3.449−01	6.897−01	26.4
51	4.645−01	9.291−01	2.323+00	4.645+00	15.6
52	6.157−01	1.231+00	3.078+00	6.157+00	6.1
53	6.157−01	1.231+00	3.078+00	6.157+00	6.1
54	6.157−01	1.231+00	3.078+00	6.157+00	6.1
55	6.157−01	1.231+00	3.078+00	6.157+00	6.1
56	1.335−03	2.670−03	6.674−03	1.335−02	43.0
57	3.588−04	7.177−04	1.794−03	3.588−03	20.6
58	3.588−04	7.177−04	1.794−03	3.588−03	20.6
59	3.588−04	7.177−04	1.794−03	3.588−03	20.6
60	3.588−04	7.177−04	1.794−03	3.588−03	20.6
61	2.168+00	4.337+00	1.084+01	2.168+01	2.5
62	2.168+00	4.337+00	1.084+01	2.168+01	2.5
63	2.168+00	4.337+00	1.084+01	2.168+01	2.5
64	2.168+00	4.337+00	1.084+01	2.168+01	2.5
65	1.711−02	3.422−02	8.556−02	1.711−01	13.0
66	1.711−02	3.422−02	8.556−02	1.711−01	13.0
67	1.711−02	3.422−02	8.556−02	1.711−01	13.0
68	1.711−02	3.422−02	8.556−02	1.711−01	13.0

Table 16

Total Dose (in rads) due to a 10 keV Temperature Blackbody X-Ray Source Located Directly in Front of the SBI Weapon Platform

Detector Region	Exterior Wall Loading 1 cal/cm^2	2 cal/cm^2	5 cal/cm^2	10 cal/cm^2	% FSD
1	4.127+00[a]	8.255+00	2.064+01	4.127+01	16.7
2	7.569+01	1.514+02	3.785+02	7.569+02	2.0
3	6.609+01	1.322+02	3.305+02	6.609+02	3.0
4	7.569+01	1.514+02	3.785+02	7.569+02	2.0
5	7.569+01	1.514+02	3.785+02	7.569+02	2.0
6	6.609+01	1.322+02	3.305+02	6.609+02	3.0
7	7.569+01	1.514+02	3.785+02	7.569+02	2.0
8	2.559+01	5.118+01	1.279+02	2.559+02	2.0
9	2.559+01	5.118+01	1.279+02	2.559+02	2.0
10	2.559+01	5.118+01	1.279+02	2.559+02	2.0
11	2.559+01	5.118+01	1.279+02	2.559+02	2.0
12	2.559+01	5.118+01	1.279+02	2.559+02	2.0
13	2.559+01	5.118+01	1.279+02	2.559+02	2.0
14	2.559+01	5.118+01	1.279+02	2.559+02	2.0
15	2.559+01	5.118+01	1.279+02	2.559+02	2.0
16	5.602+00	1.120+01	2.801+01	5.602+01	11.3
17	6.142+00	1.228+01	3.071+01	6.142+01	5.3
18	6.142+00	1.228+01	3.071+01	6.142+01	5.3
19	6.142+00	1.228+01	3.071+01	6.142+01	5.3
20	6.142+00	1.228+01	3.071+01	6.142+01	5.3
21	1.920−02	3.839−02	9.599−02	1.920−01	30.6
22	2.834−03	5.669−03	1.417−02	2.834−02	36.8
23	2.834−03	5.669−03	1.417−02	2.834−02	36.8
24	2.834−03	5.669−03	1.417−02	2.834−02	36.8
25	2.834−03	5.669−03	1.417−02	2.834−02	36.8
26	6.185+01	1.237+02	3.092+02	6.185+02	3.9
27	6.287+01	1.257+02	3.143+02	6.287+02	1.1
28	6.287+01	1.257+02	3.143+02	6.287+02	1.1
29	6.287+01	1.257+02	3.143+02	6.287+02	1.1
30	6.287+01	1.257+02	3.143+02	6.287+02	1.1
31	1.771−01	3.541−01	8.853−01	1.771+00	33.3
32	9.216−02	1.843−01	4.608−01	9.216−01	18.6
33	9.216−02	1.843−01	4.608−01	9.216−01	18.6
34	9.216−02	1.843−01	4.608−01	9.216−01	18.6
35	9.216−02	1.843−01	4.608−01	9.216−01	18.6

[a]Read as 4.127×10^0.

Table 16 - continued

Detector Region	Exterior Wall Loading 1 cal/cm^2	2 cal/cm^2	5 cal/cm^2	10 cal/cm^2	% FSD
36	8.107−02	1.621−01	4.053−01	8.107−01	14.4
37	4.927−02	9.853−02	2.463−01	4.927−01	17.7
38	7.681−02	1.536−01	3.840−01	7.681−01	18.5
39	4.307−02	8.614−02	2.154−01	4.307−01	13.5
40	1.523−01	3.047−01	7.617−01	1.523+00	16.2
41	8.107−02	1.621−01	4.053−01	8.107−01	14.4
42	4.927−02	9.853−02	2.463−01	4.927−01	17.7
43	7.681−02	1.536−01	3.840−01	7.681−01	18.5
44	4.307−02	8.614−02	2.154−01	4.307−01	13.5
45	1.523−01	3.047−01	7.617−01	1.523+00	16.2
46	5.599−01	1.120+00	2.800+00	5.599+00	38.2
47	4.178−01	8.356−01	2.089+00	4.178+00	51.9
48	1.431−01	2.863−01	7.156−01	1.431+00	30.9
49	7.555−01	1.511+00	3.777+00	7.555+00	32.3
50	1.899+00	3.798+00	9.495+00	1.899+01	24.6
51	5.493+00	1.099+01	2.746+01	5.493+01	9.5
52	4.589+00	9.177+00	2.294+01	4.589+01	3.4
53	4.589+00	9.177+00	2.294+01	4.589+01	3.4
54	4.589+00	9.177+00	2.294+01	4.589+01	3.4
55	4.589+00	9.177+00	2.294+01	4.589+01	3.4
56	1.219−01	2.437−01	6.093−01	1.219+00	24.8
57	4.175−02	8.351−02	2.088−01	4.175−01	10.1
58	4.175−02	8.351−02	2.088−01	4.175−01	10.1
59	4.175−02	8.351−02	2.088−01	4.175−01	10.1
60	4.175−02	8.351−02	2.088−01	4.175−01	10.1
61	6.971+00	1.394+01	3.486+01	6.971+01	1.9
62	6.971+00	1.394+01	3.486+01	6.971+01	1.9
63	6.971+00	1.394+01	3.486+01	6.971+01	1.9
64	6.971+00	1.394+01	3.486+01	6.971+01	1.9
65	2.044−01	4.089−01	1.022+00	2.044+00	7.3
66	2.044−01	4.089−01	1.022+00	2.044+00	7.3
67	2.044−01	4.089−01	1.022+00	2.044+00	7.3
68	2.044−01	4.089−01	1.022+00	2.044+00	7.3

Table 17

Total Dose (in rads) due to a 20 keV Temperature Blackbody X-Ray Source Located Directly in Front of the SBI Weapon Platform

Detector Region	Exterior Wall Loading 1 cal/cm^2	2 cal/cm^2	5 cal/cm^2	10 cal/cm^2	% FSD
1	1.784+01[a]	3.567+01	8.918+01	1.784+02	10.7
2	1.086+02	2.172+02	5.430+02	1.086+03	1.4
3	9.820+01	1.964+02	4.910+02	9.820+02	3.3
4	1.086+02	2.172+02	5.430+02	1.086+03	1.4
5	1.086+02	2.172+02	5.430+02	1.086+03	1.4
6	9.820+01	1.964+02	4.910+02	9.820+02	3.3
7	1.086+02	2.172+02	5.430+02	1.086+03	1.4
8	4.126+01	8.253+01	2.063+02	4.126+02	1.6
9	4.126+01	8.253+01	2.063+02	4.126+02	1.6
10	4.126+01	8.253+01	2.063+02	4.126+02	1.6
11	4.126+01	8.253+01	2.063+02	4.126+02	1.6
12	4.126+01	8.253+01	2.063+02	4.126+02	1.6
13	4.126+01	8.253+01	2.063+02	4.126+02	1.6
14	4.126+01	8.253+01	2.063+02	4.126+02	1.6
15	4.126+01	8.253+01	2.063+02	4.126+02	1.6
16	2.764+01	5.527+01	1.382+02	2.764+02	7.0
17	2.056+01	4.113+01	1.028+02	2.056+02	3.7
18	2.056+01	4.113+01	1.028+02	2.056+02	3.7
19	2.056+01	4.113+01	1.028+02	2.056+02	3.7
20	2.056+01	4.113+01	1.028+02	2.056+02	3.7
21	7.120−02	1.424−01	3.560−01	7.120−01	26.3
22	8.446−02	1.689−01	4.223−01	8.446−01	29.4
23	8.446−02	1.689−01	4.223−01	8.446−01	29.4
24	8.446−02	1.689−01	4.223−01	8.446−01	29.4
25	8.446−02	1.689−01	4.223−01	8.446−01	29.4
26	1.149+02	2.299+02	5.747+02	1.149+03	3.0
27	1.043+02	2.085+02	5.213+02	1.043+03	1.4
28	1.043+02	2.085+02	5.213+02	1.043+03	1.4
29	1.043+02	2.085+02	5.213+02	1.043+03	1.4
30	1.043+02	2.085+02	5.213+02	1.043+03	1.4
31	9.702−01	1.940+00	4.851+00	9.702+00	31.8
32	3.310−01	6.620−01	1.655+00	3.310+00	18.3
33	3.310−01	6.620−01	1.655+00	3.310+00	18.3
34	3.310−01	6.620−01	1.655+00	3.310+00	18.3
35	3.310−01	6.620−01	1.655+00	3.310+00	18.3

[a] Read as 1.784×10^1.

Table 17 - continued

Detector Region	Exterior Wall Loading 1 cal/cm^2	2 cal/cm^2	5 cal/cm^2	10 cal/cm^2	% FSD
36	1.424−01	2.848−01	7.121−01	1.424+00	8.6
37	1.781−01	3.561−01	8.903−01	1.781+00	9.5
38	1.667−01	3.335−01	8.337−01	1.667+00	9.5
39	1.932−01	3.863−01	9.659−01	1.932+00	8.3
40	2.369−01	4.738−01	1.185+00	2.369+00	7.9
41	1.424−01	2.848−01	7.121−01	1.424+00	8.6
42	1.781−01	3.561−01	8.903−01	1.781+00	9.5
43	1.667−01	3.335−01	8.337−01	1.667+00	9.5
44	1.932−01	3.863−01	9.659−01	1.932+00	8.3
45	2.369−01	4.738−01	1.185+00	2.369+00	7.9
46	6.888−01	1.378+00	3.444+00	6.888+00	19.5
47	3.068+00	6.136+00	1.534+01	3.068+01	24.1
48	4.468−01	8.937−01	2.234+00	4.468+00	36.5
49	2.828+00	5.656+00	1.414+01	2.828+01	22.1
50	6.426−01	1.285+00	3.213+00	6.426+00	26.6
51	1.383+01	2.767+01	6.917+01	1.383+02	4.7
52	1.246+01	2.492+01	6.231+01	1.246+02	2.4
53	1.246+01	2.492+01	6.231+01	1.246+02	2.4
54	1.246+01	2.492+01	6.231+01	1.246+02	2.4
55	1.246+01	2.492+01	6.231+01	1.246+02	2.4
56	1.015+00	2.029+00	5.073+00	1.015+01	15.6
57	4.546−01	9.091−01	2.273+00	4.546+00	8.8
58	4.546−01	9.091−01	2.273+00	4.546+00	8.8
59	4.546−01	9.091−01	2.273+00	4.546+00	8.8
60	4.546−01	9.091−01	2.273+00	4.546+00	8.8
61	1.028+01	2.056+01	5.140+01	1.028+02	1.3
62	1.028+01	2.056+01	5.140+01	1.028+02	1.3
63	1.028+01	2.056+01	5.140+01	1.028+02	1.3
64	1.028+01	2.056+01	5.140+01	1.028+02	1.3
65	8.325−01	1.665+00	4.163+00	8.325+00	3.9
66	8.325−01	1.665+00	4.163+00	8.325+00	3.9
67	8.325−01	1.665+00	4.163+00	8.325+00	3.9
68	8.325−01	1.665+00	4.163+00	8.325+00	3.9

Table 18

Dose (in rads-cm^2/X-Ray) to the SBI Weapon Platform for Various Temperature Blackbody X-Ray Sources Located at a 45 Degree Angle to the Top/Front Face of the SBI Weapon Platform

Detector Region	Temperature of Blackbody Source 2 keV	5 keV	10 keV	20 keV
1	0.000+00 ± 0.0	1.699−16[a] ± 48.8[b]	6.408−15 ± 30.8	5.273−14 ± 14.5
2	2.431−20 ± 51.9	4.101−16 ± 22.9	1.012−14 ± 11.0	5.474−14 ± 8.9
3	0.000+00 ± 0.0	2.926−17 ± 29.5	2.561−15 ± 21.3	2.743−14 ± 13.4
4	2.431−20 ± 51.9	4.101−16 ± 22.9	1.012−14 ± 11.0	5.474−14 ± 8.9
5	3.954−19 ± 38.1	6.563−16 ± 17.3	1.674−14 ± 10.9	9.581−14 ± 6.2
6	6.257−20 ± 44.8	9.917−16 ± 22.6	2.884−14 ± 8.9	1.398−13 ± 6.2
7	3.954−19 ± 38.1	6.563−16 ± 17.3	1.674−14 ± 10.9	9.581−14 ± 6.2
8	3.071−20 ± 53.7	1.895−16 ± 14.9	7.868−15 ± 7.9	4.779−14 ± 9.2
9	3.755−21 ± 99.9	1.676−16 ± 23.5	3.474−15 ± 16.6	2.958−14 ± 6.0
10	3.755−21 ± 99.9	1.676−16 ± 23.5	3.474−15 ± 16.6	2.958−14 ± 6.0
11	3.071−20 ± 53.7	1.895−16 ± 14.9	7.868−15 ± 7.9	4.779−14 ± 9.2
12	2.265−19 ± 29.1	1.529−15 ± 9.2	2.837−14 ± 9.0	1.296−13 ± 4.7
13	2.343−18 ± 26.2	4.799−15 ± 6.8	6.939−14 ± 3.0	2.774−13 ± 4.5
14	2.343−18 ± 26.2	4.799−15 ± 6.8	6.939−14 ± 3.0	2.774−13 ± 4.5
15	2.265−19 ± 29.1	1.529−15 ± 9.2	2.837−14 ± 9.0	1.296−13 ± 4.7
16	1.813−20 ± 66.7	1.542−16 ± 31.0	8.004−15 ± 18.9	5.823−14 ± 15.2
17	0.000+00 ± 0.0	9.208−17 ± 48.0	5.544−15 ± 20.8	2.795−14 ± 11.3
18	1.174−18 ± 32.0	2.575−15 ± 18.7	4.495−14 ± 7.3	2.411−13 ± 6.5
19	2.042−19 ± 37.5	9.936−16 ± 13.8	2.888−14 ± 7.2	1.259−13 ± 7.1
20	2.042−19 ± 37.5	9.936−16 ± 13.8	2.888−14 ± 7.2	1.259−13 ± 7.1
21	6.034−20 ± 66.7	5.038−17 ± 30.6	2.581−15 ± 24.0	2.983−14 ± 15.4
22	0.000+00 ± 0.0	1.056−17 ± 38.1	1.398−15 ± 39.4	1.380−14 ± 21.6
23	7.034−19 ± 39.7	3.723−15 ± 15.7	4.580−14 ± 10.3	2.344−13 ± 7.6
24	1.775−19 ± 31.1	1.276−15 ± 11.5	2.340−14 ± 7.0	1.112−13 ± 4.6
25	1.775−19 ± 31.1	1.276−15 ± 11.5	2.340−14 ± 7.0	1.112−13 ± 4.6
26	1.336−19 ± 52.0	1.511−15 ± 14.4	3.235−14 ± 9.0	1.837−13 ± 6.0
27	6.670−19 ± 65.2	1.269−15 ± 5.8	2.936−14 ± 8.7	1.398−13 ± 4.7
28	2.037−18 ± 32.7	4.292−15 ± 11.1	7.435−14 ± 4.4	2.709−13 ± 4.2
29	8.642−19 ± 22.8	2.201−15 ± 7.1	3.679−14 ± 5.3	1.797−13 ± 4.0
30	8.642−19 ± 22.8	2.201−15 ± 7.1	3.679−14 ± 5.3	1.797−13 ± 4.0
31	3.279−20 ± 61.8	1.745−16 ± 22.7	3.977−15 ± 14.3	3.432−14 ± 12.6
32	0.000+00 ± 0.0	5.512−18 ± 70.8	8.687−16 ± 27.7	7.873−15 ± 18.2
33	1.216−18 ± 28.4	3.273−15 ± 8.1	5.752−14 ± 5.7	2.143−13 ± 4.2
34	1.282−19 ± 24.5	1.433−15 ± 6.1	2.513−14 ± 7.4	1.205−13 ± 4.4
35	1.282−19 ± 24.5	1.433−15 ± 6.1	2.513−14 ± 7.4	1.205−13 ± 4.4

[a] Read as 1.699×10^{-16}.
[b] Percent Fractional Standard Deviation.

Table 18 - continued

Detector Region	Temperature of Blackbody Source 2 keV	5 keV	10 keV	20 keV
36	8.302−15 ± 5.9	1.748−13 ± 2.2	3.418−13 ± 5.1	4.068−13 ± 4.6
37	1.285−14 ± 5.2	1.882−13 ± 2.4	3.662−13 ± 3.3	4.467−13 ± 5.3
38	2.188−14 ± 4.0	2.172−13 ± 2.3	3.859−13 ± 3.2	4.575−13 ± 4.4
39	6.090−14 ± 3.2	3.547−13 ± 1.9	4.396−13 ± 3.8	4.846−13 ± 2.9
40	7.426−13 ± 0.5	9.183−13 ± 1.0	5.887−13 ± 2.9	5.069−13 ± 3.9
41	8.302−15 ± 5.9	1.748−13 ± 2.2	3.418−13 ± 5.1	4.068−13 ± 4.6
42	1.285−14 ± 5.2	1.882−13 ± 2.4	3.662−13 ± 3.3	4.467−13 ± 5.3
43	2.188−14 ± 4.0	2.172−13 ± 2.3	3.859−13 ± 3.2	4.575−13 ± 4.4
44	6.090−14 ± 3.2	3.547−13 ± 1.9	4.396−13 ± 3.8	4.846−13 ± 2.9
45	7.426−13 ± 0.5	9.183−13 ± 1.0	5.887−13 ± 2.9	5.069−13 ± 3.9
46	1.257−17 ± 22.1	2.344−14 ± 6.9	2.068−13 ± 7.2	5.998−13 ± 3.1
47	4.261−17 ± 14.2	3.096−14 ± 8.8	2.399−13 ± 5.2	6.021−13 ± 5.1
48	1.932−16 ± 10.7	5.226−14 ± 10.6	3.346−13 ± 3.5	6.427−13 ± 4.6
49	1.197−15 ± 8.4	1.409−13 ± 3.8	5.011−13 ± 3.5	8.425−13 ± 3.7
50	6.207−13 ± 1.0	1.363−12 ± 1.2	1.496−12 ± 2.1	1.419−12 ± 2.7
51	5.331−20 ± 48.2	1.000−16 ± 60.3	2.115−15 ± 15.7	1.953−14 ± 6.0
52	0.000+00 ± 0.0	1.729−17 ± 35.3	1.056−15 ± 25.6	7.588−15 ± 11.6
53	7.046−19 ± 20.9	1.366−15 ± 10.1	2.131−14 ± 8.1	1.064−13 ± 5.6
54	6.479−20 ± 28.0	5.098−16 ± 13.4	1.035−14 ± 7.3	5.285−14 ± 3.3
55	6.479−20 ± 28.0	5.098−16 ± 13.4	1.035−14 ± 7.3	5.285−14 ± 3.3
56	1.107−20 ± 98.8	8.247−17 ± 54.5	1.938−15 ± 14.8	2.384−14 ± 7.5
57	0.000+00 ± 0.0	1.273−17 ± 64.1	1.340−16 ± 24.7	5.950−15 ± 19.3
58	4.366−20 ± 62.9	2.156−16 ± 29.4	5.959−15 ± 13.8	3.962−14 ± 8.6
59	1.135−19 ± 23.6	4.130−16 ± 13.6	9.471−15 ± 7.3	5.065−14 ± 3.8
60	1.135−19 ± 23.6	4.130−16 ± 13.6	9.471−15 ± 7.3	5.065−14 ± 3.8
61	2.202−18 ± 18.4	6.935−16 ± 5.9	7.889−15 ± 4.7	3.742−14 ± 2.6
62	2.202−18 ± 18.4	6.935−16 ± 5.9	7.889−15 ± 4.7	3.742−14 ± 2.6
63	3.641−18 ± 14.1	2.453−15 ± 5.2	2.724−14 ± 1.8	1.128−13 ± 1.6
64	3.641−18 ± 14.1	2.453−15 ± 5.2	2.724−14 ± 1.8	1.128−13 ± 1.6
65	9.992−23 ± 81.5	1.856−17 ± 26.2	8.766−16 ± 9.9	7.165−15 ± 4.4
66	9.992−23 ± 81.5	1.856−17 ± 26.2	8.766−16 ± 9.9	7.165−15 ± 4.4
67	1.626−18 ± 10.1	1.740−15 ± 3.9	2.111−14 ± 2.9	9.657−14 ± 2.0
68	1.626−18 ± 10.1	1.740−15 ± 3.9	2.111−14 ± 2.9	9.657−14 ± 2.0

Table 19

Total Dose (in rads) due to a 2 keV Temperature Blackbody X-Ray Source Located at a 45 Degree Angle to the Top/Front Face of the SBI Weapon Platform

Detector	Exterior Wall Loading				
Region	1 cal/cm^2	2 cal/cm^2	5 cal/cm^2	10 cal/cm^2	% FSD
1	0.000+00	0.000+00	0.000+00	0.000+00	0.0
2	1.181−04[a]	2.362−04	5.905−04	1.181−03	51.9
3	0.000+00	0.000+00	0.000+00	0.000+00	0.0
4	1.181−04	2.362−04	5.905−04	1.181−03	51.9
5	1.920−03	3.841−03	9.601−03	1.920−02	38.1
6	3.039−04	6.078−04	1.520−03	3.039−03	44.8
7	1.920−03	3.841−03	9.601−03	1.920−02	38.1
8	1.492−04	2.983−04	7.458−04	1.492−03	53.7
9	1.824−05	3.648−05	9.120−05	1.824−04	100.0
10	1.824−05	3.648−05	9.120−05	1.824−04	100.0
11	1.492−04	2.983−04	7.458−04	1.492−03	53.7
12	1.100−03	2.200−03	5.500−03	1.100−02	29.1
13	1.138−02	2.276−02	5.691−02	1.138−01	26.2
14	1.138−02	2.276−02	5.691−02	1.138−01	26.2
15	1.100−03	2.200−03	5.500−03	1.100−02	29.1
16	8.804−05	1.761−04	4.402−04	8.804−04	66.7
17	0.000+00	0.000+00	0.000+00	0.000+00	0.0
18	5.701−03	1.140−02	2.851−02	5.701−02	32.0
19	9.917−04	1.983−03	4.959−03	9.917−03	37.5
20	9.917−04	1.983−03	4.959−03	9.917−03	37.5
21	2.931−04	5.862−04	1.465−03	2.931−03	66.7
22	0.000+00	0.000+00	0.000+00	0.000+00	0.0
23	3.416−03	6.833−03	1.708−02	3.416−02	39.7
24	8.623−04	1.725−03	4.311−03	8.623−03	31.1
25	8.623−04	1.725−03	4.311−03	8.623−03	31.1
26	6.489−04	1.298−03	3.245−03	6.489−03	52.0
27	3.240−03	6.480−03	1.620−02	3.240−02	65.2
28	9.895−03	1.979−02	4.947−02	9.895−02	32.7
29	4.197−03	8.395−03	2.099−02	4.197−02	22.8
30	4.197−03	8.395−03	2.099−02	4.197−02	22.8
31	1.592−04	3.185−04	7.962−04	1.592−03	61.8
32	0.000+00	0.000+00	0.000+00	0.000+00	0.0
33	5.905−03	1.181−02	2.952−02	5.905−02	28.4
34	6.227−04	1.245−03	3.114−03	6.227−03	24.5
35	6.227−04	1.245−03	3.114−03	6.227−03	24.5

[a]Read as 1.181×10^{-4}.

Table 19 - continued

Detector Region	Exterior Wall Loading 1 cal/cm^2	2 cal/cm^2	5 cal/cm^2	10 cal/cm^2	% FSD
36	4.032+01	8.065+01	2.016+02	4.032+02	5.9
37	6.244+01	1.249+02	3.122+02	6.244+02	5.2
38	1.063+02	2.126+02	5.314+02	1.063+03	4.0
39	2.958+02	5.916+02	1.479+03	2.958+03	3.2
40	3.607+03	7.214+03	1.803+04	3.607+04	.5
41	4.032+01	8.065+01	2.016+02	4.032+02	5.9
42	6.244+01	1.249+02	3.122+02	6.244+02	5.2
43	1.063+02	2.126+02	5.314+02	1.063+03	4.0
44	2.958+02	5.916+02	1.479+03	2.958+03	3.2
45	3.607+03	7.214+03	1.803+04	3.607+04	.5
46	6.106−02	1.221−01	3.053−01	6.106−01	22.1
47	2.070−01	4.139−01	1.035+00	2.070+00	14.2
48	9.383−01	1.877+00	4.692+00	9.383+00	10.7
49	5.816+00	1.163+01	2.908+01	5.816+01	8.4
50	3.015+03	6.030+03	1.507+04	3.015+04	1.0
51	2.589−04	5.178−04	1.295−03	2.589−03	48.2
52	0.000+00	0.000+00	0.000+00	0.000+00	0.0
53	3.422−03	6.845−03	1.711−02	3.422−02	20.9
54	3.147−04	6.294−04	1.573−03	3.147−03	28.0
55	3.147−04	6.294−04	1.573−03	3.147−03	28.0
56	5.378−05	1.076−04	2.689−04	5.378−04	98.8
57	0.000+00	0.000+00	0.000+00	0.000+00	0.0
58	2.121−04	4.241−04	1.060−03	2.121−03	62.9
59	5.512−04	1.102−03	2.756−03	5.512−03	23.6
60	5.512−04	1.102−03	2.756−03	5.512−03	23.6
61	1.070−02	2.139−02	5.348−02	1.070−01	18.4
62	1.070−02	2.139−02	5.348−02	1.070−01	18.4
63	1.769−02	3.537−02	8.843−02	1.769−01	14.1
64	1.769−02	3.537−02	8.843−02	1.769−01	14.1
65	4.853−07	9.706−07	2.427−06	4.853−06	81.5
66	4.853−07	9.706−07	2.427−06	4.853−06	81.5
67	7.896−03	1.579−02	3.948−02	7.896−02	10.1
68	7.896−03	1.579−02	3.948−02	7.896−02	10.1

Table 20

Total Dose (in rads) due to a 5 keV Temperature Blackbody X-Ray Source Located at a 45 Degree Angle to the Top/Front Face of the SBI Weapon Platform

Detector	Exterior Wall Loading				
Region	1 cal/cm^2	2 cal/cm^2	5 cal/cm^2	10 cal/cm^2	% FSD
1	3.289−01[a]	6.577−01	1.644+00	3.289+00	48.8
2	7.937−01	1.587+00	3.969+00	7.937+00	22.9
3	5.663−02	1.133−01	2.832−01	5.663−01	29.5
4	7.937−01	1.587+00	3.969+00	7.937+00	22.9
5	1.270+00	2.540+00	6.350+00	1.270+01	17.3
6	1.919+00	3.839+00	9.596+00	1.919+01	22.6
7	1.270+00	2.540+00	6.350+00	1.270+01	17.3
8	3.667−01	7.333−01	1.833+00	3.667+00	14.9
9	3.244−01	6.488−01	1.622+00	3.244+00	23.5
10	3.244−01	6.488−01	1.622+00	3.244+00	23.5
11	3.667−01	7.333−01	1.833+00	3.667+00	14.9
12	2.958+00	5.917+00	1.479+01	2.958+01	9.2
13	9.287+00	1.857+01	4.644+01	9.287+01	6.8
14	9.287+00	1.857+01	4.644+01	9.287+01	6.8
15	2.958+00	5.917+00	1.479+01	2.958+01	9.2
16	2.985−01	5.970−01	1.492+00	2.985+00	31.0
17	1.782−01	3.564−01	8.910−01	1.782+00	48.0
18	4.983+00	9.966+00	2.491+01	4.983+01	18.7
19	1.923+00	3.846+00	9.614+00	1.923+01	13.8
20	1.923+00	3.846+00	9.614+00	1.923+01	13.8
21	9.751−02	1.950−01	4.875−01	9.751−01	30.6
22	2.043−02	4.087−02	1.022−01	2.043−01	38.1
23	7.204+00	1.441+01	3.602+01	7.204+01	15.7
24	2.470+00	4.940+00	1.235+01	2.470+01	11.5
25	2.470+00	4.940+00	1.235+01	2.470+01	11.5
26	2.923+00	5.847+00	1.462+01	2.923+01	14.4
27	2.456+00	4.912+00	1.228+01	2.456+01	5.8
28	8.306+00	1.661+01	4.153+01	8.306+01	11.1
29	4.259+00	8.519+00	2.130+01	4.259+01	7.1
30	4.259+00	8.519+00	2.130+01	4.259+01	7.1
31	3.377−01	6.754−01	1.689+00	3.377+00	22.7
32	1.067−02	2.133−02	5.333−02	1.067−01	70.8
33	6.334+00	1.267+01	3.167+01	6.334+01	8.1
34	2.773+00	5.545+00	1.386+01	2.773+01	6.1
35	2.773+00	5.545+00	1.386+01	2.773+01	6.1

[a]Read as 3.289×10^{-1}.

Table 20 - continued

Detector	Exterior Wall Loading				
Region	1 cal/cm^2	2 cal/cm^2	5 cal/cm^2	10 cal/cm^2	% FSD
36	3.383+02	6.765+02	1.691+03	3.383+03	2.2
37	3.643+02	7.285+02	1.821+03	3.643+03	2.4
38	4.203+02	8.406+02	2.102+03	4.203+03	2.3
39	6.864+02	1.373+03	3.432+03	6.864+03	1.9
40	1.777+03	3.554+03	8.886+03	1.777+04	1.0
41	3.383+02	6.765+02	1.691+03	3.383+03	2.2
42	3.643+02	7.285+02	1.821+03	3.643+03	2.4
43	4.203+02	8.406+02	2.102+03	4.203+03	2.3
44	6.864+02	1.373+03	3.432+03	6.864+03	1.9
45	1.777+03	3.554+03	8.886+03	1.777+04	1.0
46	4.536+01	9.073+01	2.268+02	4.536+02	6.9
47	5.992+01	1.198+02	2.996+02	5.992+02	8.8
48	1.011+02	2.023+02	5.057+02	1.011+03	10.6
49	2.727+02	5.454+02	1.364+03	2.727+03	3.8
50	2.638+03	5.276+03	1.319+04	2.638+04	1.2
51	1.935−01	3.871−01	9.676−01	1.935+00	60.3
52	3.346−02	6.693−02	1.673−01	3.346−01	35.3
53	2.643+00	5.286+00	1.322+01	2.643+01	10.1
54	9.866−01	1.973+00	4.933+00	9.866+00	13.4
55	9.866−01	1.973+00	4.933+00	9.866+00	13.4
56	1.596−01	3.192−01	7.980−01	1.596+00	54.5
57	2.463−02	4.926−02	1.232−01	2.463−01	64.1
58	4.172−01	8.344−01	2.086+00	4.172+00	29.4
59	7.993−01	1.599+00	3.997+00	7.993+00	13.6
60	7.993−01	1.599+00	3.997+00	7.993+00	13.6
61	1.342+00	2.684+00	6.711+00	1.342+01	5.9
62	1.342+00	2.684+00	6.711+00	1.342+01	5.9
63	4.747+00	9.495+00	2.374+01	4.747+01	5.2
64	4.747+00	9.495+00	2.374+01	4.747+01	5.2
65	3.591−02	7.182−02	1.795−01	3.591−01	26.2
66	3.591−02	7.182−02	1.795−01	3.591−01	26.2
67	3.367+00	6.734+00	1.684+01	3.367+01	3.9
68	3.367+00	6.734+00	1.684+01	3.367+01	3.9

Table 21

Total Dose (in rads) due to a 10 keV Temperature Blackbody X-Ray Source Located at a 45 Degree Angle to the Top/Front Face of the SBI Weapon Platform

Detector Region	Exterior Wall Loading 1 cal/cm^2	2 cal/cm^2	5 cal/cm^2	10 cal/cm^2	% FSD
1	6.198+00[a]	1.240+01	3.099+01	6.198+01	30.8
2	9.787+00	1.957+01	4.893+01	9.787+01	11.0
3	2.477+00	4.955+00	1.239+01	2.477+01	21.3
4	9.787+00	1.957+01	4.893+01	9.787+01	11.0
5	1.619+01	3.239+01	8.097+01	1.619+02	10.9
6	2.790+01	5.579+01	1.395+02	2.790+02	8.9
7	1.619+01	3.239+01	8.097+01	1.619+02	10.9
8	7.610+00	1.522+01	3.805+01	7.610+01	7.9
9	3.360+00	6.720+00	1.680+01	3.360+01	16.6
10	3.360+00	6.720+00	1.680+01	3.360+01	16.6
11	7.610+00	1.522+01	3.805+01	7.610+01	7.9
12	2.744+01	5.488+01	1.372+02	2.744+02	9.0
13	6.712+01	1.342+02	3.356+02	6.712+02	3.0
14	6.712+01	1.342+02	3.356+02	6.712+02	3.0
15	2.744+01	5.488+01	1.372+02	2.744+02	9.0
16	7.742+00	1.548+01	3.871+01	7.742+01	18.9
17	5.363+00	1.073+01	2.681+01	5.363+01	20.8
18	4.348+01	8.695+01	2.174+02	4.348+02	7.3
19	2.794+01	5.587+01	1.397+02	2.794+02	7.2
20	2.794+01	5.587+01	1.397+02	2.794+02	7.2
21	2.497+00	4.993+00	1.248+01	2.497+01	24.0
22	1.352+00	2.705+00	6.762+00	1.352+01	39.4
23	4.430+01	8.860+01	2.215+02	4.430+02	10.3
24	2.264+01	4.527+01	1.132+02	2.264+02	7.0
25	2.264+01	4.527+01	1.132+02	2.264+02	7.0
26	3.130+01	6.259+01	1.565+02	3.130+02	9.0
27	2.840+01	5.680+01	1.420+02	2.840+02	8.7
28	7.192+01	1.438+02	3.596+02	7.192+02	4.4
29	3.558+01	7.116+01	1.779+02	3.558+02	5.3
30	3.558+01	7.116+01	1.779+02	3.558+02	5.3
31	3.847+00	7.693+00	1.923+01	3.847+01	14.3
32	8.402−01	1.680+00	4.201+00	8.402+00	27.7
33	5.563+01	1.113+02	2.782+02	5.563+02	5.7
34	2.431+01	4.862+01	1.216+02	2.431+02	7.4
35	2.431+01	4.862+01	1.216+02	2.431+02	7.4

[a]Read as 6.198×10^0.

Table 21 - continued

Detector Region	Exterior Wall Loading 1 cal/cm^2	2 cal/cm^2	5 cal/cm^2	10 cal/cm^2	% FSD
36	3.306+02	6.613+02	1.653+03	3.306+03	5.1
37	3.542+02	7.085+02	1.771+03	3.542+03	3.3
38	3.733+02	7.465+02	1.866+03	3.733+03	3.2
39	4.252+02	8.505+02	2.126+03	4.252+03	3.8
40	5.694+02	1.139+03	2.847+03	5.694+03	2.9
41	3.306+02	6.613+02	1.653+03	3.306+03	5.1
42	3.542+02	7.085+02	1.771+03	3.542+03	3.3
43	3.733+02	7.465+02	1.866+03	3.733+03	3.2
44	4.252+02	8.505+02	2.126+03	4.252+03	3.8
45	5.694+02	1.139+03	2.847+03	5.694+03	2.9
46	2.000+02	4.001+02	1.000+03	2.000+03	7.2
47	2.321+02	4.642+02	1.160+03	2.321+03	5.2
48	3.236+02	6.472+02	1.618+03	3.236+03	3.5
49	4.847+02	9.694+02	2.423+03	4.847+03	3.5
50	1.447+03	2.893+03	7.233+03	1.447+04	2.1
51	2.046+00	4.092+00	1.023+01	2.046+01	15.7
52	1.022+00	2.043+00	5.108+00	1.022+01	25.6
53	2.061+01	4.122+01	1.030+02	2.061+02	8.1
54	1.002+01	2.003+01	5.008+01	1.002+02	7.3
55	1.002+01	2.003+01	5.008+01	1.002+02	7.3
56	1.874+00	3.749+00	9.372+00	1.874+01	14.8
57	1.296−01	2.592−01	6.479−01	1.296+00	24.7
58	5.764+00	1.153+01	2.882+01	5.764+01	13.8
59	9.162+00	1.832+01	4.581+01	9.162+01	7.3
60	9.162+00	1.832+01	4.581+01	9.162+01	7.3
61	7.631+00	1.526+01	3.815+01	7.631+01	4.7
62	7.631+00	1.526+01	3.815+01	7.631+01	4.7
63	2.634+01	5.269+01	1.317+02	2.634+02	1.8
64	2.634+01	5.269+01	1.317+02	2.634+02	1.8
65	8.479−01	1.696+00	4.240+00	8.479+00	9.9
66	8.479−01	1.696+00	4.240+00	8.479+00	9.9
67	2.042+01	4.085+01	1.021+02	2.042+02	2.9
68	2.042+01	4.085+01	1.021+02	2.042+02	2.9

Table 22

Total Dose (in rads) due to a 20 keV Temperature Blackbody X-Ray Source Located at a 45 Degree Angle to the Top/Front Face of the SBI Weapon Platform

Detector	Exterior Wall Loading				
Region	1 cal/cm^2	2 cal/cm^2	5 cal/cm^2	10 cal/cm^2	% FSD
1	2.550+01[a]	5.100+01	1.275+02	2.550+02	14.5
2	2.647+01	5.295+01	1.324+02	2.647+02	8.9
3	1.327+01	2.654+01	6.634+01	1.327+02	13.4
4	2.647+01	5.295+01	1.324+02	2.647+02	8.9
5	4.634+01	9.268+01	2.317+02	4.634+02	6.2
6	6.759+01	1.352+02	3.380+02	6.759+02	6.2
7	4.634+01	9.268+01	2.317+02	4.634+02	6.2
8	2.311+01	4.623+01	1.156+02	2.311+02	9.2
9	1.431+01	2.861+01	7.153+01	1.431+02	6.0
10	1.431+01	2.861+01	7.153+01	1.431+02	6.0
11	2.311+01	4.623+01	1.156+02	2.311+02	9.2
12	6.270+01	1.254+02	3.135+02	6.270+02	4.7
13	1.342+02	2.683+02	6.708+02	1.342+03	4.5
14	1.342+02	2.683+02	6.708+02	1.342+03	4.5
15	6.270+01	1.254+02	3.135+02	6.270+02	4.7
16	2.816+01	5.632+01	1.408+02	2.816+02	15.2
17	1.352+01	2.704+01	6.760+01	1.352+02	11.3
18	1.166+02	2.332+02	5.830+02	1.166+03	6.5
19	6.090+01	1.218+02	3.045+02	6.090+02	7.1
20	6.090+01	1.218+02	3.045+02	6.090+02	7.1
21	1.443+01	2.885+01	7.214+01	1.443+02	15.4
22	6.672+00	1.334+01	3.336+01	6.672+01	21.6
23	1.134+02	2.267+02	5.668+02	1.134+03	7.6
24	5.379+01	1.076+02	2.690+02	5.379+02	4.6
25	5.379+01	1.076+02	2.690+02	5.379+02	4.6
26	8.883+01	1.777+02	4.442+02	8.883+02	6.0
27	6.759+01	1.352+02	3.379+02	6.759+02	4.7
28	1.310+02	2.621+02	6.552+02	1.310+03	4.2
29	8.692+01	1.738+02	4.346+02	8.692+02	4.0
30	8.692+01	1.738+02	4.346+02	8.692+02	4.0
31	1.660+01	3.320+01	8.299+01	1.660+02	12.6
32	3.808+00	7.615+00	1.904+01	3.808+01	18.2
33	1.036+02	2.073+02	5.181+02	1.036+03	4.2
34	5.826+01	1.165+02	2.913+02	5.826+02	4.4
35	5.826+01	1.165+02	2.913+02	5.826+02	4.4

[a]Read as 2.550×10^1.

Table 22 - continued

Detector Region	Exterior Wall Loading 1 cal/cm^2	2 cal/cm^2	5 cal/cm^2	10 cal/cm^2	% FSD
36	1.968+02	3.935+02	9.838+02	1.968+03	4.6
37	2.160+02	4.321+02	1.080+03	2.160+03	5.3
38	2.213+02	4.425+02	1.106+03	2.213+03	4.4
39	2.343+02	4.687+02	1.172+03	2.343+03	2.9
40	2.451+02	4.903+02	1.226+03	2.451+03	3.9
41	1.968+02	3.935+02	9.838+02	1.968+03	4.6
42	2.160+02	4.321+02	1.080+03	2.160+03	5.3
43	2.213+02	4.425+02	1.106+03	2.213+03	4.4
44	2.343+02	4.687+02	1.172+03	2.343+03	2.9
45	2.451+02	4.903+02	1.226+03	2.451+03	3.9
46	2.901+02	5.802+02	1.451+03	2.901+03	3.1
47	2.912+02	5.824+02	1.456+03	2.912+03	5.1
48	3.108+02	6.217+02	1.554+03	3.108+03	4.6
49	4.074+02	8.149+02	2.037+03	4.074+03	3.7
50	6.864+02	1.373+03	3.432+03	6.864+03	2.7
51	9.443+00	1.889+01	4.721+01	9.443+01	6.0
52	3.670+00	7.340+00	1.835+01	3.670+01	11.6
53	5.145+01	1.029+02	2.573+02	5.145+02	5.6
54	2.556+01	5.112+01	1.278+02	2.556+02	3.3
55	2.556+01	5.112+01	1.278+02	2.556+02	3.3
56	1.153+01	2.306+01	5.765+01	1.153+02	7.5
57	2.877+00	5.755+00	1.439+01	2.877+01	19.3
58	1.916+01	3.833+01	9.582+01	1.916+02	8.6
59	2.449+01	4.899+01	1.225+02	2.449+02	3.8
60	2.449+01	4.899+01	1.225+02	2.449+02	3.8
61	1.810+01	3.620+01	9.049+01	1.810+02	2.6
62	1.810+01	3.620+01	9.049+01	1.810+02	2.6
63	5.453+01	1.091+02	2.726+02	5.453+02	1.6
64	5.453+01	1.091+02	2.726+02	5.453+02	1.6
65	3.465+00	6.931+00	1.733+01	3.465+01	4.4
66	3.465+00	6.931+00	1.733+01	3.465+01	4.4
67	4.670+01	9.341+01	2.335+02	4.670+02	2.0
68	4.670+01	9.341+01	2.335+02	4.670+02	2.0

4. SUMMARY AND CONCLUSIONS

The calculations and results described in this report represent the efforts of an initial study to assess the effects and magnitude of X–ray radiation from nuclear weapon detonations on the performance of a representative Space Based Interceptor weapon platform. The platform configuration in this work contained only a thin laser shield and no kinetic energy weapon shield or internal shielding. This yielded data on the radiation response of the components and surface materials and hardening requirements of the platform itself.

The majority of radiation from a nuclear weapon is in the form of X–rays which impact on the surface of the platform in the form of an energetic hydrodynamic-like impulse and, depending on the blackbody temperature of the weapon, deliver large doses to on-board electronic equipment. Surface damage will generally predominate. The single event upset and latch-up rates in vital circuits from nuclear weapon X–ray radiation may cause mission failure for weapon platforms that are near the limit of the wall loadings suggested (less than 10 cal/cm^2). The solar panels and the BSTS, SSTS antenna dose profiles exhibit a sharp decline at the lower temperature spectra (four orders of magnitude at 1 keV) and relatively flat distributions at the higher temperature spectra (less than 20% at 20 keV). The dose to the outer shell of the solar panels and antenna for the 1, 2, and 5 keV devices is sufficiently large enough to cause permanent damage to the electronics. Further analysis with smaller thicknesses needs to be performed to determine surface effects (blow–off, melting, etc.) present for the 1, 2, and 5 keV source spectra.

The dose to the sensitive components within the exterior hull of the platform was not sufficient to cause any damage at a 1 cal/cm^2 exterior wall loading. At higher wall loadings, some of the KKV computers and sensors begin to receive doses large enough to cause damage. Furthermore, the majority of the dose to the internal components of the SBI platform came from blackbody devices with temperatures greater than 10 keV. The low temperature devices will yield a higher flux of X–rays, but the incident energy will be insufficient to cause permanent damage to the internal electronic components.

The analysis presented in this work focused on the total dose (in units of rads or rads $\cdot$ cm^2/X-ray) received by the various components on board the SBI weapon platform without regard to the rate at which the dose was received. As stated above, generally the total dose to the sensitive components within the exterior hull of the platform was not sufficient enough to cause any damage at a 1 cal/cm^2 exterior wall loading. However, a typical weapon detonation releases the X-ray radiation in a pulse with a width on the order of 10–40 nanosecond. Therefore, if a 40 nanosecond pulse width is assumed, all of the total dose results would have to be multiplied by 2.5×10^7 sec^{-1} to obtain the dose rate (Gamma dot) results. This would yield dose rates to the sensitive components in the range of 10^8–10^{12} rads/sec which could be large enough to cause damage. Consequently, the dose rate becomes the primary mode of failure even though the total dose is not large enough to cause any damage to the sensitive components. In this case, additional shielding around the sensitive components would be required.

The platform geometry considered in this study did not account for the presence of additional shielding material present between the X–ray radiation source and the sensitive platform component. The effects of shielding from within the platform architecture is seen by the different dose levels received in the KKVs and fuel tanks. Because of the low dose levels to the components within the exterior hull of the platform, no additional shielding is required. However, sensors and electronic components on the surface or outside of the exterior hull will require some form of X–ray shielding to survive the effects of a weapon detonation yielding a wall loading of 1 cal/cm^2 or greater.

The results reported here are for a single weapon detonation and for wall loadings less than 10 cal/cm^2. No consideration was given to multiple bursts wherein the structural integrity of the platform could be violated or the single event/latch-up rate is prohibitive.

Finally, it should be noted that all of the results reported here were obtained using available response functions for dose, damage, single-event upset, etc. Some of the damage response data require re-evaluation and updating to reduce the uncertainties in the results which may be as large as a factor of two for the present data.

5. ACKNOWLEDGMENTS

The authors wish to thank Mrs. Dawn C. Human for her significant efforts in typing this manuscript and for her assistance throughout this program.

REFERENCES

1. L. W. Ricketts, "Fundamentals of Nuclear Hardening of Electronic Equipment," Wiley–Nterscience, New York, NY, 1972.
2. MAJ R. Leong, 1LT D. Lahti, 1LT K. Murphy, 1LT S. Rieco, and 1LT R. Zacharko, "AFWL Exoatmospheric Nuclear Radiation Environment Prediction and Shielding Codes Applicable to the Strategic Defense Initiative (SDI)," Draft Report, Air Force Weapons Laboratory, Kirtland Air Force Base, New Mexico, 87117.
3. J. M. Barnes, R. T. Santoro, J. O. Johnson, J. D. Drischler, T. A. Gabriel, and M. S. Smith, "Shield Optimization Program, Part II: Effects of Van Allen Belt Radiation on SDI Weapon Platforms," Oak Ridge National Laboratory, ORNL/TM-10957, 1988.
4. R. Seigel and John R. Howell, "Thermal Radiation Heat Transfer," McGraw-Hill, Inc., 1972.
5. W. R. Nelson, H. Hirayama, and D. W. O. Rogers, "The EGS4 Code System," SLAC-265, Stanford Linear Accelerator Center, 1985.
6. T. A. Gabriel, J. O. Johnson, and B. L. Bishop, "CALOR89, A Code Package for the Design of Calorimeter Systems," ORNL/TM in preparation.

INTERNAL DISTRIBUTION

1. R. G. Alsmiller, Jr.
2. B. R. Appleton
3. D. E. Bartine
4–8. J. M. Barnes
9. T. J. Burns
10. R. M. Davis
11. J. B. Dooley
12–16. J. D. Drischler
17–21. T. A. Gabriel
22. C. M. Haaland
23. E. B. Harris
24. D. T. Ingersoll
25–29. J. O. Johnson
30. R. A. Lillie
31. F. C. Maienschein
32. J. R. Merriman
33. W. L. Roberts
34. R. W. Roussin
35–39. R. T. Santoro
40–44. M. S. Smith
45. D. G. Thomas
46. R. C. Ward
47. C. R. Weisbin
48. EPMD Reports Office
49–50. Laboratory Records Department
51. Laboratory Records, ORNL–RC
52. Document Reference Section
53. Central Research Library
54. ORNL Patent Section

EXTERNAL DISTRIBUTION

55. Dr. Charles Aeby, AFWL/NTC, Air Force Weapons Laboratory, Kirtland Air Force Base, New Mexico 87117-6008
56. Lt Dale Atkinson, AFWL/NTCA, Air Force Weapons Laboratory, Kirtland Air Force Base, New Mexico 87117-6008
57. J. J. Dorning, Department of Nuclear Engineering and Engineering Physics, Thornton Hall, University of Virginia, Charlottesville, Virginia 22901
58. Lt Richard Engstrom, AFWL/NTCA, Air Force Weapons Laboratory, Kirtland Air Force Base, Albuquerque, New Mexico 87117
59. R. M. Haralick, Department of Electrical Engineering, University of Washington, Seattle, Washington 98195
60. Office of the Assistant Manager for Energy Research and Development, Department of Energy, Oak Ridge Operations, P.O. Box 2001, Oak Ridge, TN 37831
61–70. Office of Scientific and Technical Information, P.O. Box 62, Oak Ridge, Tennessee 37830